

Project Number: <KLB-1702>

Design of a Biaxial Test Device to Measure Soft Tissue Properties

A Major Qualifying Project Report:
Submitted to the Faculty
of the
WORCESTER POLYTECHNIC INSTITUTE

In partial fulfillment of the requirements for the
Degree of Bachelor of Science

Submitted by:

Alexandra Chretien

Melissa Daigle

Allison Hacker

Bridget Rinkel

Date: April 26, 2018

Approved:

Prof. Kristen L. Billiar, Advisor

Table of Contents

Table of Figures	4
Table of Tables	6
Authorship.....	7
Acknowledgments.....	8
Abstract.....	9
1. Introduction.....	10
2. Literature Review.....	12
2.1 Medical Significance	12
2.2 Soft Tissue	13
2.3 Biaxial Testing.....	15
2.4 Gripping Mechanisms.....	17
Clamps	18
Sutures.....	19
Rakes.....	20
2.5 Current Market Devices and Gold Standards	20
CellScale	21
Instron-Sacks Planar Biaxial Soft Tissue Testing System.....	25
3. Project Strategy.....	27
3.1 Initial and Revised Client Statement.....	27
3.2 Technical Design Requirements	28
Objectives	28
Constraints	29
Functions.....	30
Specifications	30
Functional Blocks	31
3.3 Standard Design Requirements.....	32
3.4 Management Approach.....	34
General Project Approach.....	34
Background Research	35
Idea Generation and Evaluation.....	36
Prototyping.....	37

Financial Statement.....	37
4. Design Process	39
4.1 Needs Analysis.....	39
4.2 Concept Maps and Designs/Prototyping/Feasibility Studies	41
Velcro.....	42
Setting.....	43
Grips.....	44
4.3 Alternative Designs.....	48
4.4 Final Design Selection	53
Gripping Mechanism	53
Loading Tools	58
5. Final Design Verification.....	63
5.1 Shear Evaluation	63
5.2 Lateral Movement Evaluation.....	66
5.3 Usability.....	68
6. Final Design Validation	70
6.1 Feedback on Final Design.....	70
6.2 Economics and Manufacturability	70
6.3 Environmental Impact.....	72
6.4 Societal and Political Concerns	72
6.5 Ethical Concerns	73
6.6 Health and Safety Issues	73
6.7 Sustainability.....	73
7. Discussion.....	75
7.1 Shear Evaluation	75
7.2 Lateral movement	76
7.3 Usability.....	76
8. Conclusions and Recommendations	77
References.....	79
Glossary	82
Appendix A:.....	84
Appendix B:.....	88
Appendix C:.....	91
Appendix D:.....	94

Appendix E:	98
Appendix F.....	101

Table of Figures

Figure 2.1: Fiber orientation of soft tissue showing unidirectional alignment, intra-lamellar alignment, and interspersed alignment [10].	13
Figure 2.2: Typical Force-Displacement Curve for Soft Tissue [11].	14
Figure 2.3: Illustration of uniaxial testing (left) vs. biaxial testing (right).	14
Figure 2.4: A schematic of the basic components of a biaxial test device [1].	16
Figure 2.5: Specimen deformation vs. gripping mechanism [15].	17
Figure 2.6: Representation of CellScale’s Biorakes.	23
Figure 2.7: Representation of CellScale’s Balanced Pulley mounting system.	24
Figure 2.8: Representation of CellScale’s Clamp mounting system on a cruciform test specimen [20].	24
Figure 3.1: Gantt Chart for Design Process	35
Figure 4.1: Crucial components for consideration of the current device at WPI (left). The cruciform-shaped bath (center) and the bearings (right).	41
Figure 4.2: Uniaxial Instron test of hydrated rice paper with Velcro grips	43
Figure 4.3: Uniaxial tensile testing of hydrated rice paper using sutures	46
Figure 4.4: Stainless Steel Braided Wire Rake Prototype	47
Figure 4.5: Uniaxial test of hydrated rice paper using initial rake prototype design	47
Figure 4.6: The first alternative design idea - Stage Design	49
Figure 4.7: Alternative grip design - Paired pivots	49
Figure 4.8: Alternative grip design - Circular base design	50
Figure 4.9: (left) Alternative grip design - Chairlift design, (right) bearing pole on existing device	51
Figure 4.10: Alternative loading tool - Tine spacer	52
Figure 4.11: Alternative loading tool design - Platform tool	52
Figure 4.12: First prototype of the final grip design produced on a large scale. The tines are 1.5mm diameter stainless steel mounted in a 0.95 cm thickness base of UHMWPE	56
Figure 4.13: Second prototype of the final grip design produced on a smaller scale. The tines are 0.6mm diameter stainless steel mounted in a 0.95 cm thickness base of UHMWPE	56

Figure 4.14: : Final grip design using a 3D printed stage of low-friction nylon with four stainless steel quilter’s pin tines	57
Figure 4.15: First prototype of tine spacers and loading platform.....	60
Figure 4.16: Second iteration of tine spacers.....	61
Figure 4.17: Final iteration of loading tools including both tine spacers and load platform (Shown from left to right, the load platform is lowered onto the tines, aligned by the tine spacer. The top piece of the platform is lifted by the handle, and the bottom piece is removed from the long handle, leaving the specimen mount on the rake tines).....	61
Figure 4.18: Varying dimensions for tine spacers and load platform to incorporate a range of specimens (Represented on the left is a medium sized load platform spaced for a 1.75 cm x 1.75 cm sample, in the middle is a load platform for a smaller 1 cm x 1 cm sample with angled grooves, and on the right for a large sample of 2.5 cm x 2.5 cm with angled grooves).....	62
Figure 5.1: Force-displacement curves for biaxial testing of anisotropic gauze with fibers angled 45 degrees from the X axis.....	64
Figure 5.2: Average force-displacement curves for biaxial testing of anisotropic gauze with fibers aligned along the X axis.....	64
Figure 5.3: Anisotropic gauze before testing (left) and after testing (right) with fixed rakes.....	65
Figure 5.4: Anisotropic gauze before testing (left) and after testing (right) with pivoting rakes.....	66
Figure 5.5: Lateral Movement Evaluation Schematic	68
Figure 5.6: : Preliminary usability trial with all components of the system aligned.....	69

Table of Tables

Table 2.1: CellScale’s BioTester Capabilities	22
Table 2.2: Specifications of Instron-Sacks Biaxial Test Device.....	25
Table 3.1: Design Function/Means	32
Table 4.1: Pairwise Comparison Chart of Attachment System Objectives.....	40
Table 4.2: Weighted Grip Design Comparison Matrix.....	54
Table 4.3: Weighted Loading Mechanism Design Comparison Matrix	58
Table 5.1: Bending Calculations of a Fixed Tine	67

Authorship

Acknowledgments: MD

Abstract: MD

1. Introduction: AC, MD, AH, BR
2. Literature Review
 - 2.1 Medical Significance: MD, AC
 - 2.2: Soft Tissue: AC, MD, AH
 - 2.3 Biaxial Testing: AH, MD
 - 2.4 Current Market Devices and Gold Standards: BR, MD
 - 2.5 Gripping Mechanisms: AC, MD, BR
3. Project Strategy
 - 3.1 Initial and Revised Client Statement: AC, MD
 - 3.2 Technical Design Requirements: AC, MD, AH, BR
 - 3.3 Standard Design Requirements: AC, MD, AH, BR
 - 3.4 Management Approach: AC, MD, AH, BR
4. Design Process
 - 4.1 Needs Analysis: AC, MD, AH, BR
 - 4.2 Concept Maps and Designs/Prototyping/Feasibility Studies: AC, MD, AH, BR
 - 4.3 Alternative Designs: AC, BR
 - 4.4 Final Design: MD, AH, AC
5. Design Verification
 - 5.1 Shear Evaluation: MD, BR, AC
 - 5.2 Lateral Movement Evaluation: MD
 - 5.3 Usability: MD, AH
6. Final Design and Validation: AH
7. Discussion
 - 7.1 Shear Evaluation: MD, AH, BR
 - 7.2 Lateral Movement Evaluation: MD, AH
 - 7.3 Usability: MD
8. Conclusion: BR, AC

Acknowledgments

We would like to thank project advisor Kristen Billiar, and project mentor Ying Lei, for their continued help and support throughout this design project. We would also like to recognize Biomedical Engineering graduate student Elizabeth English, for her assistance and fabrication of the fibrin microthread and hydrogel cardiac patches necessary for the design verification stage of this project.

We would also like to thank application scientist Erica Stults, and senior application scientist Adriana Hera, in Information Technology at WPI for their support and knowledge in 3D printing and LabVIEW. Additionally, the team received considerable assistance from Ian Anderson, Senior Instructional Laboratory Technician for Washburn Machine Shops at WPI, in the manufacturing and refining of the design prototypes. The team also discussed device hardware and software updates at length with David Melendez, US Account Manager for National Instruments, and would like to recognize his help in evaluating the performance of the device and consideration of future recommendations.

Lastly, the team would like to recognize Glenn Gaudette, Professor of Biomedical Engineering at WPI as an invaluable resource for information in tissue engineering and cardiac tissue regeneration pertinent to the successful function of this design.

Abstract

Biaxial testing is needed to evaluate the varying mechanical properties of fibrous soft tissue. A current gap in technology fails to effectively grip tissue so that each axis of load can behave independently of the other, while allowing an easy attachment method. The goal of this project was to develop a gripping and loading system that would allow force distribution, preserve the specimen, and have high usability. Using rapid prototyping, a gripping and loading mechanism was developed for a biaxial test device at WPI. Through the use of force distribution calculations and experimental testing, comparisons to current technology were made. From these results, the team can conclude that the objectives were met.

1. Introduction

Tissue engineering is a branch of regenerative medicine that aims to synthesize materials that function like biological soft tissue to replace or repair those of diseased or damaged organs. Soft tissue is a pseudoplastic and anisotropic material that is flexible and has soft mechanical properties. Anisotropic means that the tissue exhibits mechanical properties that differ based on the axis of load [1]. Soft tissue is constantly subjected to physical, chemical, and biological stresses so it has a dynamic structure [2]. Ideally, artificial tissue aims to mimic the mechanical properties of its respective biological tissue. To ensure that these bioengineered tissues will function successfully in the body, various mechanical properties, like tensile strength, elasticity, and compliance, must be tested to forces that the body would impart on the tissue in vivo [3]. As engineered materials aim to mimic biological tissue structure and function, these tissues often exhibit mechanical properties that vary depending upon the direction of load. To adequately quantify the anisotropic stress-strain performance of tissue engineered materials, mechanical testing must occur in multiple directions.

Biaxial testing measures the mechanical properties of both biological and engineered tissue by capturing the properties of tissue in multiple directions. These measurements provide important data on stress-strain relationships within the material, and other mechanical properties such as elasticity and compliance, and tensile strength that are necessary to improve engineered tissue to better mimic biological properties [4]. Biaxial testing has its advantages over uniaxial testing, as uniaxial tests do not sufficiently recognize the 3D behavior of the tissue.

Currently, there are various biaxial test devices on the market that measure these mechanical properties, but they are costly. CellScale and Instron are namely two of the main companies that make biaxial test devices. Both of these companies offer devices of high quality

that allow users to easily test specimens to obtain more accurate data than could be obtained through uniaxial testing. Worcester Polytechnic Institute (WPI) also owns a similar device that was engineered by a student team in 2005. It offers similar capabilities to marketed devices; however, all of these devices lack an ideal gripping mechanism to effectively measure the properties of compliant tissue. The current methods of specimen attachment within these devices include clamps, rakes, and suture/pulley systems. Though each of these methods are currently used today, each method has specific limitations that prevent effective attachment of soft tissue and comprehensive evaluation of mechanical properties.

The overall objective of this project is to improve WPI's biaxial test device to effectively load and grip very compliant tissue. Biaxial testing offers a unique challenge in attachment as each axis must behave independently of the other without influence of the grips for effective testing. To achieve this goal, the team developed a complete loading and attachment system that allows for lateral movement and shear in a sample, that is easy to use to test compliant tissue.

2. Literature Review

2.1 Medical Significance

The need for artificial engineered tissue is critical in the United States. There are millions of connective tissue diseases and injuries that require treatment. For example, millions of people worldwide suffer from heart failure [5]. Heart failure occurs when healthy heart muscle dies. Unlike other tissues in the body, the heart cannot regenerate functional cardiac tissue. Instead, the heart repairs the injury with scar tissue that is unable to contact or conduct electrical signals to the rest of the organ like the surrounding cardiac muscle. In this case, the scar tissue is unable to achieve the necessary mechanical properties to mimic the native tissue, resulting in loss of function and ultimately heart failure [6].

Tissue engineering is a promising field of growing research that has the potential to effectively treat many connective tissue problems, such as heart failure. One growing area of research includes the development of a cardiac heart patch intended to repair the injured heart tissue by matching the mechanical properties of healthy biological tissue. The patch is implanted over the injury to restore conduction of electrical signals and muscle contraction. However, the evaluation of these needed mechanical properties is critical to the success of such a patch. A patch that is too stiff restricts contractions that pump blood to the rest of the body. A patch that is too compliant fails to provide adequate support needed within the heart to circulate blood. To ensure these vital properties are met, cardiac patches and all other engineered artificial tissue must be tested mechanically to evaluate their ability to perform their intended functions [7].

2.2 Soft Tissue

Mimicking the biological environment when testing artificial tissue is important to ensure it will perform well in the body. Because tissues in the body are constantly subjected to a variety of physical, chemical, and biological stresses, every tissue structure is dynamic. Most soft tissue, like cardiac tissue is anisotropic, meaning varying fiber orientations in the tissue contribute to differing mechanical properties depending on the direction of an applied load [8], as seen in Fig. 2.1. Soft tissues also exhibit viscoelasticity, hysteresis, and stress relaxation, enhancing the tendency of the tissue to produce nonlinear stress-strain relationships [9].

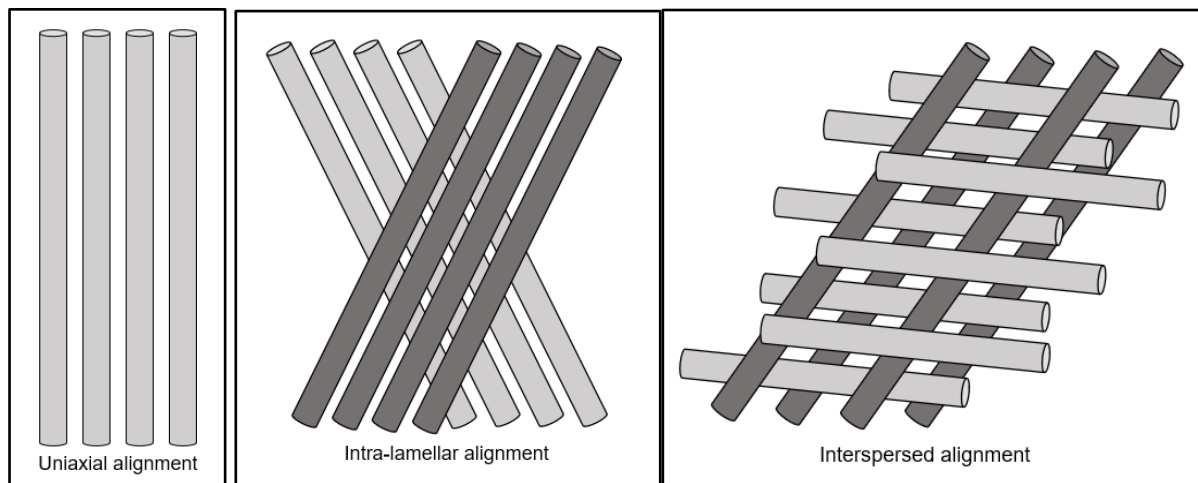


Figure 2.1: Fiber orientation of soft tissue showing unidirectional alignment, intra-lamellar alignment, and interspersed alignment [10].

An example of this non-linear behavior can be seen by the typical force-displacement curve for soft tissue shown in Fig. 2.2. This image graphs the variation in displacement depending on direction of the force applied. In a mechanical test, the loading of the sample can be equivalent in both directions (equibiaxial loading), proportional between directions (proportional loading), or independent from direction (general/non-equibiaxial loading) [11].

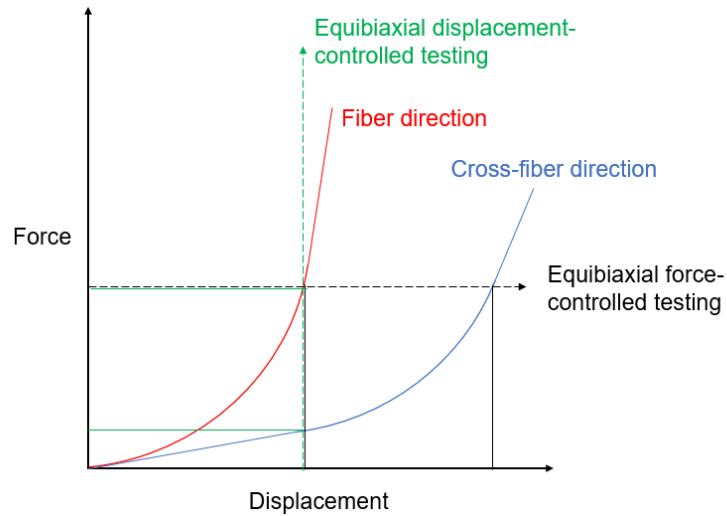


Figure 2.2: Typical Force-Displacement Curve for Soft Tissue [11].

The most common method of mechanical testing is done uniaxially in which a specimen is clamped on two ends and a load is applied along one axis, illustrated in Fig. 2.3. However, both biological and engineered tissue are often anisotropic due to varying fiber alignments, exhibiting various mechanical properties in different directions. Additionally, these tissues are intended for use in the body where they will be loaded in multiple directions. Uniaxial testing is limited to evaluating tissue in one direction and fails to incorporate any multiaxial evaluations crucial to characterizing the tissue's comprehensive mechanical properties [12].

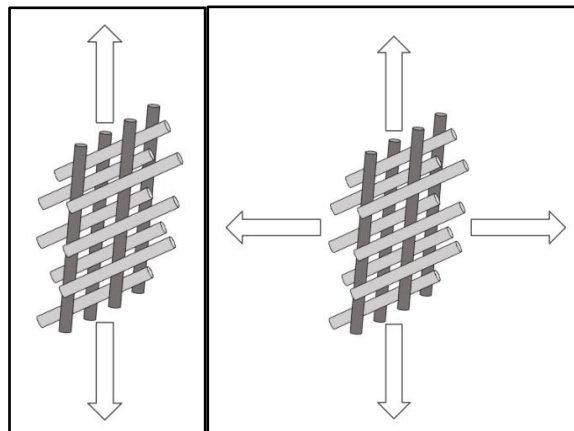


Figure 2.3: Illustration of uniaxial testing (left) vs. biaxial testing (right).

2.3 Biaxial Testing

Biaxial testing is needed to develop constitutive models of biological and bio-engineered soft tissue [9]. Constitutive models are crucial to the accurate analysis of the mechanical properties of soft tissue. These models and analysis provide critical information for the development and fabrication of synthetic soft tissue to successfully mimic biological tissue properties [4].

Although biaxial testing is superior to uniaxial testing in determining the properties of soft tissues, it poses its own challenges. Biaxial testing is much more complex than uniaxial testing as there exists a need to control two boundary conditions corresponding to the two axes. Additionally, the attachment method must also move freely in the lateral direction [9]. Modeling tissue property using planar biaxial testing cannot completely capture the three-dimensional properties of anisotropic soft tissue; however, there are various other biaxial tests to fill in these gaps [9], [13]. These tests include inflation and extension biaxial tests and equibiaxial stretching tests [13]. Additional challenges to evaluating soft tissue include small specimen size due to limited sources, difficulty gripping due to the delicate structure, and difficulty in inducing strain within the center of the sample due to high stress concentrations at the attachment sites [9]. Several current devices aim to overcome these challenges in various ways as detailed in Section 2.5.

Biaxial testing typically follows the same procedure regardless of the device. A schematic of the basic biaxial test setup is shown in Fig. 2.4. There are four main components in a biaxial test device:

1. Force Mechanism: Force is controlled and produced through the use of force transducers partnered with a servo motor and load cell [14]. Force transducers vary in nominal force

range, resolution, and overload protection depending on the intended use of the device. A detailed background on the mechanisms of force transducers can be seen in Appendix A.

2. Displacement Measurement: Displacement is measured optically to avoid mechanical error and interference with the fragile specimen [1], [9]. Optical software is typically used with a programmable CCD camera to measure the displacement in both axis directions [1]. From displacement, strain in the specimen is then estimated.
3. Environment: The specimen should be submerged in a pH and temperature-controlled media bath, typically phosphate-buffered saline (PBS) that simulates a physiological environment. To achieve *in vivo* conditions, the temperature is maintained at 37°C and the pH at approximately 7.4 [9].
4. Attachment Mechanism: The attachment method ideally distributes the applied force evenly throughout the specimen and effectively attaches the specimen to the force mechanism throughout the duration of testing [1]. Currently used attachment methods for this type of testing are detailed in Section 2.6.

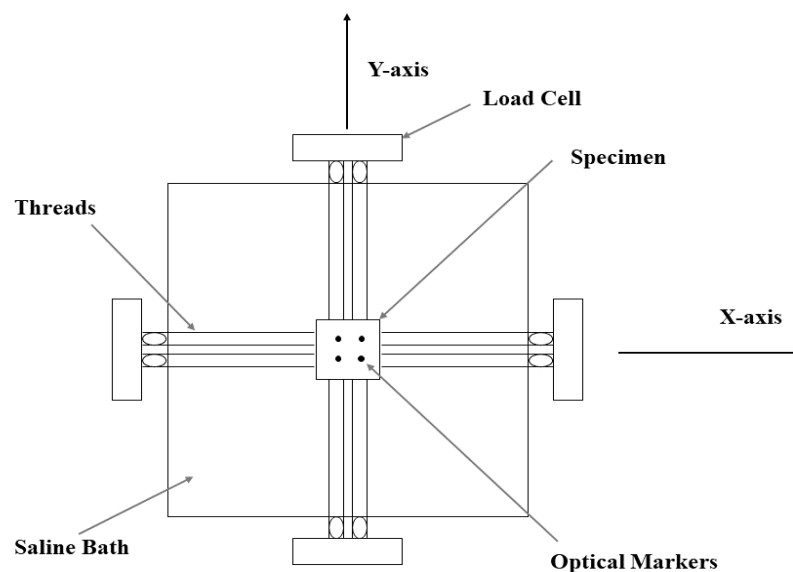


Figure 2.4: A schematic of the basic components of a biaxial test device [1].

In addition to these components, the specimen is prepared with several markers at the center of the specimen to track the displacement accurately. The displacement is tracked in the center of the specimen to mitigate any potential effects, such as stress concentrations, of the attachment method on the behavior of the tissue [9], [14]. The device typically applies the load at a set strain rate or loading rate. The device can also run based on a set stress input [12]. Other parameter inputs include preloading, stretching, holding, recovering, and resting phases [11].

2.4 Gripping Mechanisms

When designing a biaxial test device, one of the most critical aspects is determining specimen attachment. With delicate samples such as soft tissue, it is difficult to grip them properly without altering their mechanical properties or damaging the tissue. Various gripping mechanisms, shown in Fig. 2.5 below, have been constructed in previous biaxial test studies and are outlined in more detail in this section.

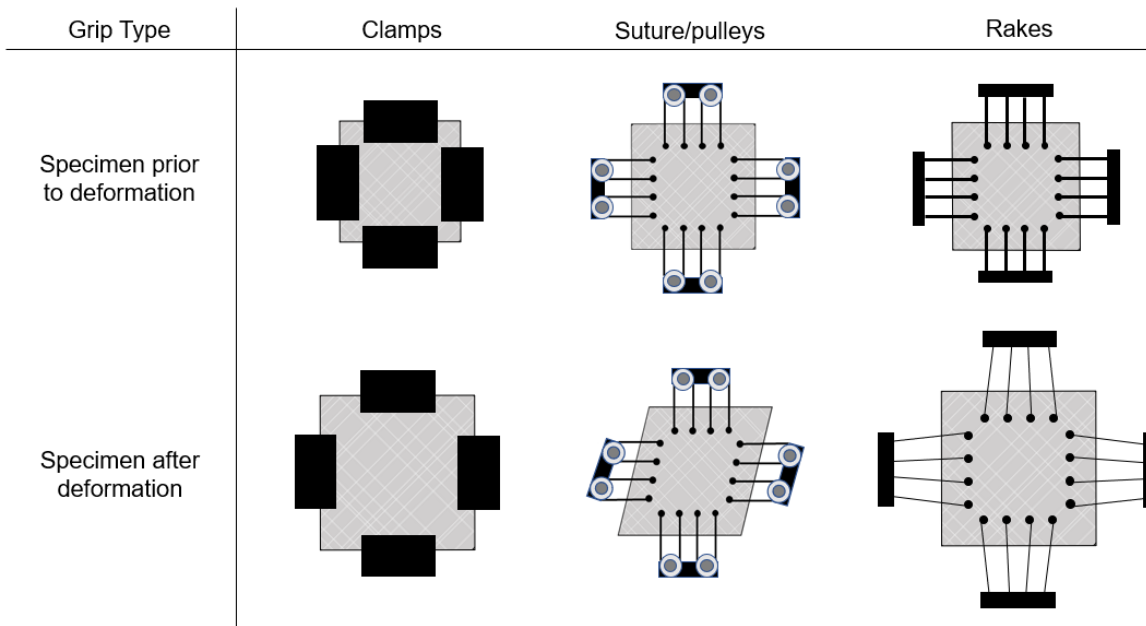


Figure 2.5: Specimen deformation vs. gripping mechanism [15].

Clamps

Clamps offer the fastest loading, highest usability, and most repeatable attachments for a tensile test; however, clamps are ideally suited for uniaxial tests. When applying a load to a compliant specimen, like soft tissue, the specimen will stretch and elongate along the axis of the load applied. Perpendicular to that axis, the specimen contracts to allow stretching with the tensile force; however, in biaxial testing, clamps also attach to the specimen along this perpendicular axis. Introducing these additional clamps often induces undesirable restriction of the specimen. For example, the specimen can no longer contract along this axis to allow for elongation in the original axis of load. Instead, the large surface area of the clamps restricts specimen movement and significantly influences the load distribution within the sample. These restrictions can lead to stress shielding and altered physical properties [15].

To mitigate this problem, an alternative specimen shape was introduced. A cruciform shaped sample allows more movement within the sample as clamps are applied to the arms and the load is distributed to the central area [16]. Testing cruciform samples over square-shaped samples results in a higher strain range and simpler data acquisition, but an inverse modeling adjustment of constitutive model parameters is needed [17]. Therefore, to utilize a clamp attachment method, researchers should prepare specimens in a cruciform shape and mathematical analysis should be altered. Additionally, this shape is extremely difficult to obtain for biological or bioengineered specimens. Both biological and artificial specimens come from limited sources, including the body or complex tissue engineering procedures. It is highly unfeasible to prepare these specimens into a cruciform shape due to limited sources, cost, and time. For these reasons, clamps are not well-suited to adequately grip anisotropic soft tissue. They offer a repeatable,

user-friendly method for a uniaxial testing grip system, but severely restrict necessary specimen stress-strain response in a biaxial test.

Sutures

Another specimen attachment method involves suturing or tethering each side of the sample to the load cell. To use this gripping mechanism, the user must be extremely cautious and gentle to securely and precisely attach the sutures without tearing the sample [18]. A typical suture-pulley test consists of a set of four sutures secured to each side of the specimen by hooks. Each suture is then looped around a pulley. This setup maintains uniform tension throughout the sample by allowing for lateral movement of the sample. Previous biaxial testing of mitral valve leaflets utilized two loops of 000 nylon suture connected to four stainless steel surgical staples. These loops encircled two stainless steel pulleys mounted on a stainless-steel ball bearing [19].

Testing with a suture and pulley system ensures uniform force is applied throughout the sample by allowing contralateral movement and rotation of the sample. An anisotropic sample may exhibit a stiffer or stronger area due to its varying fiber alignments, resulting in shear, or a geometric shift within the sample as each fiber is loaded; however, this method does not ensure uniform displacement [15]. It is also a highly variable attachment method that requires considerable time and surgical skill to attach each suture [17]. By hand, it is extremely difficult to insert the attachment hooks at precise spacing from the edges of the sample and from the other sutures. Then, looping the sutures over the pulleys may induce unwanted pre-loading to the sample and the puncture points. Therefore, the main limitations of sutures are usability, repeatability, and specimen preservation.

Rakes

A third attachment method, rakes are commonly used as a method of gripping soft tissue samples during biaxial testing. They function in a similar manner to sutures, by puncturing the specimen along the edges and attaching to the load cell. Rakes, however, do not allow for any shear available with the suturing method. The rakes are rigid tines secured by a common fixed base, driven by the load cell.

To best apply this method, research shows that increasing the number of rakes and increasing the width between rakes improves the quality of a biaxial test. The inner rakes should be as far apart as possible, and the outer rakes should be as close as possible to the adjacent rake along the additional axis. More widely spacing the load points improves the loading distribution. As the load is applied to a larger area on the specimen, stress concentrations between the puncture points are reduced [15]. The advantages of using rakes for specimen gripping include repeatability, usability, and accuracy. Hooking the rakes through the specimen requires less skill and the spacing of the rakes remains consistent from the fixed base [20]. This fixed spacing also ensures a more uniform load distribution. However, rakes may inconsistently apply the intended load as they can transfer contralateral forces onto the specimen during testing. As the rakes are fixed and extremely stiff, they offer the specimen no freedom of movement to respond anisotropically to the applied load. Consequently, they are not suitable for use in cases of large shear deformations, which are commonly seen in anisotropic specimens [15].

2.5 Current Market Devices and Gold Standards

There are currently devices available for purchase on the market that are designed for the biaxial testing of soft tissue and other biomaterials. These devices can be purchased with a

variety of grips, force transducers, or other accessories depending on specimen type. These systems can be very costly, but incorporate some design aspects worth noting.

CellScale

One biaxial device available, which can test very delicate tissue such as blood vessels, heart valves, and membranes is the BioTester, offered by CellScale. It is designed for small biomaterial and biological specimens with in-plane dimensions ranging from 3 to 15 mm. It performs biaxial testing by requesting an input of either a desired applied force or desired displacement for each axis. The software used to run the device is called LabJoy and has two modules: one module sets test parameters and one module monitors test progress. The test progress monitor includes a live video display of the test as it runs and the specimen as it deforms, which can also be replayed and accelerated or decelerated [21].

When tested, the specimen is placed in a temperature-controlled media bath. The device has four high performance actuators with in-line load cells to run a biaxial tensile test while keeping the specimen stationary. Live imaging is supplied during testing as well as real-time graphs displaying position, force, and temperature [20]. The load cells available for purchase include cells with nominal forces of 0.5 N, 1.5 N, 2.5 N, 5 N, 10 N, and 23 N, with a force accuracy of 0.2% of load cell capacity. The maximum velocity for these cells reaches 10 mm/s [22]. Each component is removable and washable, and the entire device can easily fit on a lab bench, with dimensions of 60 cm by 60 cm by 80 cm and a weight of 18 kg [20]. A list of the mechanical parts of the BioTester and their functions is included below in Table 2.1 [21], [22].

Table 2.1: CellScale's BioTester Capabilities

Equipment	Function
Camera	High resolution, CCD, synchronized video tracking and analysis
Lens	Provides illumination, high image quality
BioRake	Patented technology, quick and easy mounting of samples
Data collection	Integrated, compact, offers testing flexibility
Control	High resolution, precision measurement of small samples
USB interface	Simple, easy connection to host computer

The BioTester can determine the properties of a wide variety of samples due to the various grips it can accommodate for biaxial testing. Depending on the sample, a user can attach the specimen with either a tether mounting system, BioRakes, or clamps. These gripping mechanisms are magnetically mounted for easy interchanges between grips or for cleaning between samples [20].

Standard BioRakes consist of four grips, two for each axis. Each grip is composed of five tines attached to a common base so that one set of grips can simultaneously puncture a specimen at 20 attachment points [20]. These sets are available for purchase for \$316 [23]. Each tine of a BioRake, shown in Fig. 2.6, is electrochemically sharpened to pierce tissue samples of a wide range of toughness. The ideal specimen size compatible with this gripping mechanism is a square specimen with sides approximately 5.5 to 6 mm in length. Larger BioRakes are available for larger specimens [21]. The BioRakes are available with consistent tine spacings of 0.7 mm, 1 mm, 1.4 mm, 1.7 mm, and 2.2 mm. All of these sets, with the exception of the set with the smallest tine spacing, 0.7 mm, are 30 mm in length and 0.3 mm in diameter. The 0.7 mm spaced tines are consistent in length, at 30 mm, but have a diameter of 0.25 mm. For the BioRakes, the manual lift mechanism positions and raises the specimen into place for the insertion of the hooks

[20]. BioRakes allow for reliable repeatability, fast mounting, and uniform displacement. One drawback to this type of grip is that although there is even displacement, uniform force is not ensured throughout the specimen. These rakes are also considerably more expensive than other attachment methods.

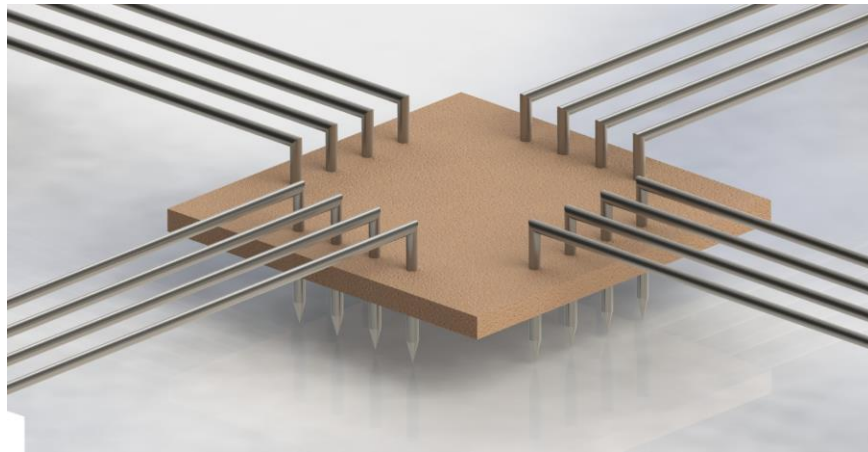


Figure 2.6: Representation of CellScale's Biorakes.

Another mechanism for specimen attachment is the balanced pulley mechanism, by which sutures are inserted into a square specimen at four points along each side. The sutures tether from the pulley to the sample using two double-ended custom suture hooks. Each of the sutures, shown in Fig. 2.7, are held at the same tension during testing as a result of a two-stage stainless steel pulley mechanism [20]. This type of grip is advantageous because it ensures the load cell induces uniform force throughout the specimen. However, it requires more time to apply the sutures and mount the specimen, and the space between sutures may not be consistent, therefore lowering attachment repeatability.

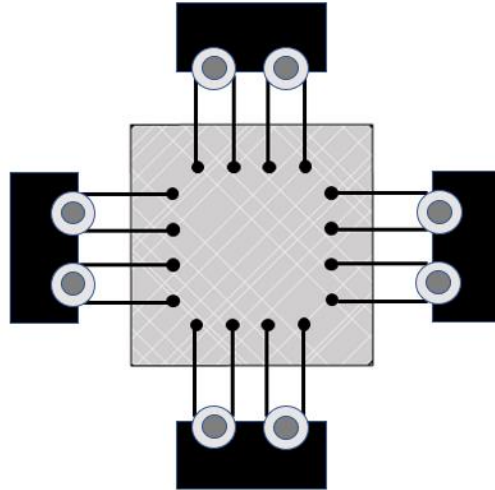


Figure 2.7: Representation of CellScale's Balanced Pulley mounting system.

CellScale also offers a clamp mounting system, shown in Fig. 2.8, which is the simplest form of specimen attachment. The stainless-steel clamps do not puncture the specimen, but rigidly clamp the four ends. Therefore, this gripping mechanism is ideal for a cruciform specimen, whose shape allows stress to distribute to the center of the specimen, rather than concentrate in the corners. This attachment method allows for fast loading and secure gripping of the specimen [20].

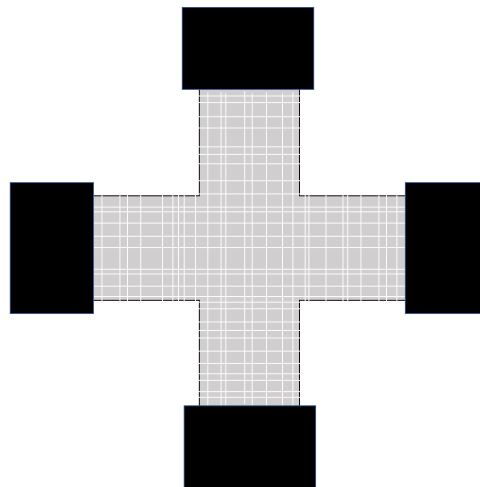


Figure 2.8: Representation of CellScale's Clamp mounting system on a cruciform test specimen [20].

The BioTester is an ideal device for testing the mechanical properties of soft tissue and has been used for various applications. This device is suitable for testing soft tissue similar to that of the lab at WPI, but costs \$80,000, which surpasses the allotted budget [23].

Instron-Sacks Planar Biaxial Soft Tissue Testing System

Instron offers a planar biaxial testing device for the characterization of natural and bioartificial soft tissue. Tests can be performed in single- or multi-axis using either position, load, or strain control [24].

The device is constructed of four Instron electromechanical MicroTester actuators and two four-axis FastTrack 8800 digital controllers. The strain measurement is accomplished through video imaging which tracks markers placed on specimen. This tracking controls the actuators based on imaged displacement and calculated strain in real-time [25]. The device comes with various accessories including a temperature-controlled saline bath, to maintain specimen hydration, clamps with adjustable grip pressure, a vibration isolation table, and a video camera, VCR, and monitor [26]. Additional specifications of this device are listed in Table 2.2 [26].

Table 2.2: Specifications of Instron-Sacks Biaxial Test Device

	Range	Accuracy	Resolution
Displacement	110 mm	0.1 μm	0.05 μm
Load Cell Set 1	5 N	0.05% of reading	0.05 N
Load Cell Set 2	500 N	0.05% of reading	5 N

This device is ideal for testing various types of soft tissue and has been used in applications such as the dynamic characterization of viscoelastic properties, assessment of reorientation of fibers under mechanical loading, the determination of mechano-structural

properties of soft tissue, and planar mechanical testing; however, this device is also extremely expensive at a cost of over \$200,000 [26].

3. Project Strategy

3.1 Initial and Revised Client Statement

The initial client statement, determined through correspondence and interviews with the client, was to design a biaxial test device to measure the mechanical properties of soft tissue such as myocardium or cardiac heart patches. After further discussion with the client and completed evaluation of the resources available to the team, the initial client statement was revised for specificity and feasibility.

The next revision of the client statement resulted in the statement, “to design or improve a biaxial test device to measure the mechanical properties of cardiac heart patches.” A previous major qualifying project team from Worcester Polytechnic Institute in 2005 created a working biaxial test device intended for mechanically testing the stress-strain behavior of artificial skin. Considering this device’s capabilities and the project budget, the team revised the client statement to include the possibility of improving this existing device. Additionally, after meeting with a graduate student interested in the adaptation of the device to test bioengineered cardiac heart patches, the team narrowed the project scope for use on low tensile strength cardiac patches.

Upon further discussion of the potential applications and improvements to the existing biaxial device, and after extensive research of the properties and characteristic of the engineered heart patches, the team revised the client statement again. This final client statement reads, “To develop a gripping mechanism and loading system for the existing biaxial test device to measure the sub-failure mechanical properties of soft tissue”. Worcester Polytechnic Institute has a faculty and student body that invests considerable time and resources into the development and research of various soft tissues and bioengineered materials for applications in tissue engineering

and regenerative medicine. To better serve this community, the team broadened the project scope from cardiac patches alone to include materials that are smaller and softer than typical anisotropic tissue. Newly engineered materials include low-layered tissue developed after less than one month. Due to the extremely low tensile strength, high modulus, and anisotropic nature of these tissues, biaxial testing is the preferred method for determining mechanical properties such as stress, strain, modulus of elasticity, and shear. A system accessible by Worcester Polytechnic Institute researchers and engineers for biaxial testing to determine these properties is needed to evaluate the ability of biomedically engineered materials to adequately mimic biological tissue *in vivo* for its intended applications, such as the replacement of diseased tissue for healthy regeneration.

3.2 Technical Design Requirements

Objectives

To address the final client statement, the project team identified the objectives of the device needed to accomplish the overarching goal. These objectives include:

1. **Force Distribution.** An effective gripping mechanism should allow for lateral movement and shear in the sample. Maximizing the lateral movement of the grips minimizes restriction of movement of the sample. Further, bending stiffness in the grips should be minimized to allow the sample to exhibit shear properties characteristic of the anisotropic material. These properties are necessary for the comprehensive study of the sample's mechanical sub-failure properties.
2. **Usability and Repeatability.** The specimen must be loaded and accurately tested by a user. To ensure that the user introduces minimal human error, such as damage to the

specimen prior to testing or inconsistent loading and/or testing of the specimen, the area of the loading stage should be large enough to allow for maneuvering and handling of the specimen. To accomplish this goal, a loading tool should fit within the bath of the device, 3.8 cm x 3.8 cm x 2.5 cm in dimension and should integrate into the biaxial testing machine without difficulty. The loading process should be repeatable, so the same test can be performed multiple times without variation. Ideally, a user can load a specimen in under one minute without damaging the specimen.

3. **Specimen Preservation.** To accurately test the sample, damage to the specimen must not be induced prior to testing. The system should limit any additional preloading of the sample. Preloading the sample may contribute to inaccurate force readings as the grips will apply a small force to the sample prior to data collection.
4. **Manufacturability.** The attachment and loading system must be easily manufacturable. The process should be repeatable, inexpensive, and compatible with the existing device. To effectively complete the project, the team must stay within the stated \$1,000 budget.

Constraints

Additionally, the team identified three main design constraints. All parts and improvements must be compatible with the existing biaxial test device, developed by the WPI major-qualifying project in 2005, to limit costs and ensure proper device function. The current device operates through LabVIEW programming, so any improvements must also be compatible with this programming. The device must also be safe for user operation, maintain the integrity of the test specimens, and demonstrate successful function, by biaxially testing the material specimen and measuring the stress-strain properties. All objectives must be met within the project timeline scheduled for completion in May 2018.

Functions

The device needs to accomplish a number of functions in order to meet the goal of allowing lateral movement and shear in the sample. It must grip the soft tissue specimens with minimal damage and biaxially test to sub-failure conditions. In order to do this, the device needs to test the specimens in two directions simultaneously so as to simulate an *in vivo* environment of multiaxial loading and biological stresses.

Additionally, the device must output the desired mechanical properties measured during testing. Sufficient data consists of force and displacement accompanied by a graph. This data allows the user to obtain any other desired values such as modulus, compliance, tensile strength, etc. with the calculations described in section 4.2. Having a visual representation of the force-displacement data gives the user an idea for the general properties of the specimen. In addition to outputting desired results, the device must require basic inputs from the user. These inputs should include length, width, and thickness of the specimen and the length of the attachment arm, as well as the strain, maximum force, etc. The device should also allow a maximum or constant stress to be inputted, to allow the user to test tissue response. This will instruct the device how to run and will ensure the accuracy of the outputs.

Specifications

This device must be able to test specimens fully within the designated ranges. Having specified limits for any device is a requirement. These limits include the size of the specimen, the range of applied forces, and the maximum strain. The maximum size specimen that this device is capable of accommodating is that of a 2.5 cm width, 2.5 cm length, and 1 mm thickness. The maximum distance this device will move in either direction is 120% of the maximum width and length of the specimen. This limit is due to the maximum strain, 120%, of the extremely elastic

soft tissue that the device can test. The maximum force this device can exert is 2N. Soft tissue varies in regard to properties, but this nominal force range accommodates most soft tissue specimens.

Functional Blocks

Some options for the shape of the specimens compatible with the device include circular, cruciform, and rectangular. While all of these shapes may not work for all types of soft tissue, they are viable options that will comply with the device.

In terms of grips, options include rakes, sutures/pulleys, clamps, and alternative methods. These types of grips are considered because they all have different benefits, whether it is ease of loading the specimen, minimum stress concentrations, or allowing lateral movement. This range of grips will be narrowed down through testing.

This device will have the capability to test both uniaxial and biaxial directions. The device can apply a tensile force in either one direction or two depending on the user's needs.

The camera and force transducers measure specific properties of the soft tissue specimens. The camera focuses on small points on the specimen and determines the deformation of the soft tissue during testing. From deformation, strain can then be estimated. The load cells apply a tensile force the sample, and the force transducers measure the corresponding response in the test material.

LabVIEW software runs the code that controls the machine. An alternative software capable of accomplishing the same goal is MATLAB, and this software may be considered or used in the event that LabVIEW is unable to successfully run the device.

A feasible list of these functions and the potential methods for accomplishing each function are organized in a functions-means table below in Table 3.1.

Table 3.1: Design Function/Means

Design Function	Means of Achieving Function		
Specimen preparation (shape)	Circular	Cruciform	Rectangular
Grip specimen	Rakes	Sutures/pulleys	Clamps
Apply tensile force	Biaxial	Uniaxial	
Force transducers	Strain gauges	Piezoelectric	Torque
Data input/output	LabVIEW	MATLAB	

3.3 Standard Design Requirements

The International Organization for Standardization, ISO, is an independent organization that creates international standards for products, services, and systems, to ensure quality, safety, and efficiency. Similarly, the ASTM is an international standards organization that develops and publishes technical standards concerning a wide range of materials, products, systems, and services. The team researched applicable ISO and ASTM standards pertaining to the biaxial testing of soft tissue and medical device testing standards. It is important to note that tissue engineering is still a developing field so standards relating to this subject may still be under development.

The team produced computer aided design models for the attachment and loading system. The ISO publishes standards associated with technical drawings, including computer aided design models, of devices and parts. These standards regulate the creation, completeness, and layout of design drawings and models for manufacturing. These considerations are necessary to follow when using 3D printing as the drawing must be detailed so that the printer can successfully print the part to the needed specifications [27].

ASTM D76 - 11 “Standard Specification for Tensile Testing Machines for Textiles” concerns the operation of tensile testing machines for the evaluation of force-displacement characteristics of fabric textiles. It includes specifications for constant rate of extension and constant rate of loading machines, like the device considered in this project. Though the primary use of this device is bioengineered and biological materials, this standard may specifically apply to operating controls of the machine [28].

Another applicable standard, ISO 376:2011 “Metallic materials — Calibration of force-proving instruments used for the verification of uniaxial testing machines” is the standard method to calibrate force-proving instruments that determine force by measuring the elastic deformation of a loaded member. This standard also provides a procedure to classify these instruments. Standardizing the calibration of force-proving devices, such as the force transducers used in the biaxial test device, allows there to be consistency of material testing and data obtained from such tests [29].

ASTM F2150 - 13 “Standard Guide for Characterization and Testing of Biomaterial Scaffolds Used in Tissue-Engineered Medical Products” is a guide containing currently available test methods for the characterization of biomaterial scaffolds used to develop and manufacture tissue-engineered medical products. The included test methods can be used to characterize bulk mechanical properties of a scaffold, such as that of bioengineered replacement tissue. As this device and this project aims to improve upon mechanical test methods of biological and replacement tissue, these test method standards may be particularly relevant [30].

Additionally, ISO 7198:2016 “Cardiovascular implants and extracorporeal systems — vascular prostheses — tubular vascular grafts and vascular patches” sets standards for evaluating vascular prostheses, their associated design attributes, and nomenclature. This standard is used

for vascular patches constructed for repair of the vascular system and includes the test methods required for the process of designing the graft materials. This standard can be applied to the design of the bioengineered materials that may be tested within our biaxial device. The standard test methods included in ISO 7198:2016 may be important considerations in the testing ranges and specifications of the biaxial device so as to satisfy test requirements identified in the standard to evaluate and verify bioengineered vascular grafts [31].

An ASTM standard that is relevant to this project is ASTM F2258 “Tensile Strength of Tissue Adhesives Test Equipment”. Its purpose is to outline a procedure to contrast the strength of tissue adhesives for use on soft tissue, as well as for quality control when creating tissue adhesive based medical devices. This standard can be applied to possible materials and adhesives to be applied to the edges of soft tissue for attachment to grips in biaxial test devices. Similarly, another ASTM standard that can be applied to this project is ASTM 52458 “Wound Strength Tissue Adhesives Sealant Test Equipment” [32].

3.4 Management Approach

General Project Approach

To complete our design objectives as determined by the client statement, the team developed the following approach scheduled over the course of the year. This schedule is intended to evaluate the improvements to the biaxial test device with the necessary dimensions, force range, gripping and loading mechanisms, and sensitivity, while remaining within budget.

Throughout the 2017-2018 academic year, the team created various preliminary designs to compare and evaluate before determining a final design. A Gantt chart was created to outline project objectives with specific dates to ensure project needs are completed on time. The Gantt

chart, shown in Fig. 3.1, schedules the team tasks, categorized by main project milestones, with specific deadlines for completion.

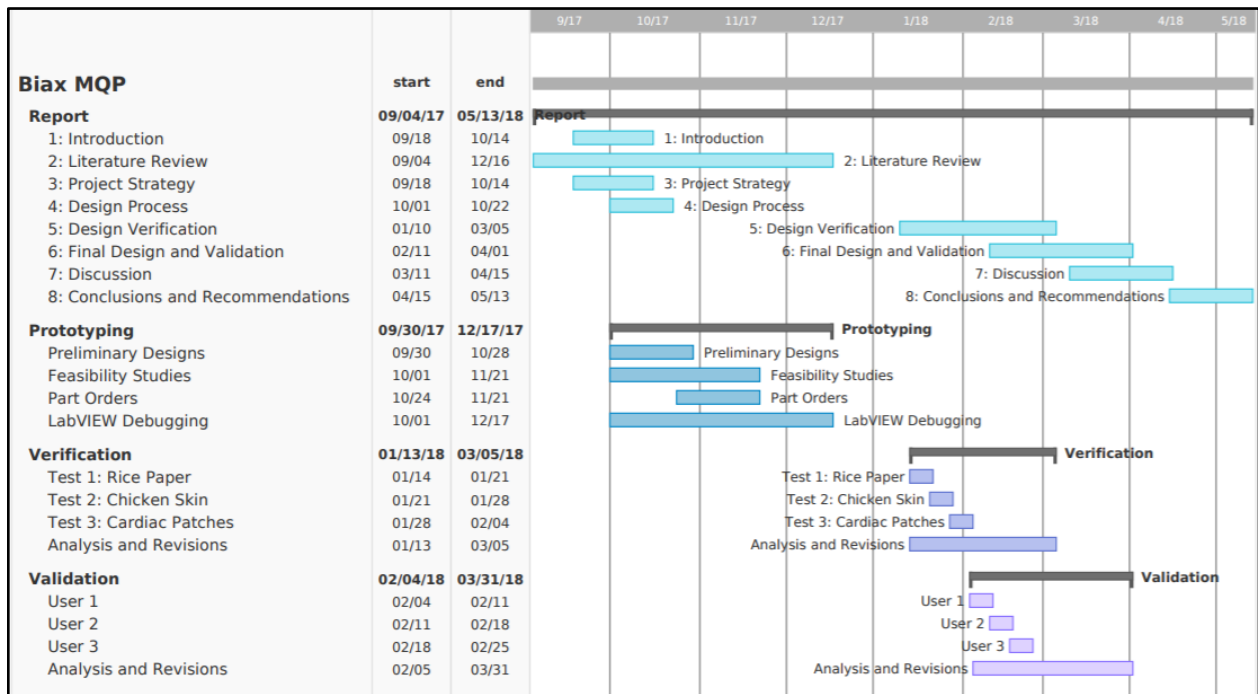


Figure 3.1: Gantt Chart for Design Process

Background Research

To design a biaxial test device to measure the mechanical properties of extremely delicate anisotropic soft tissue, the team decided it was first necessary to conduct comprehensive background research concerning biaxial testing and soft tissue. The team researched the properties and formation process of anisotropic soft tissue. It is necessary to define the range of mechanical properties of this tissue, as well as general deformation characteristics in order to determine the specifications the device must accommodate. The team also evaluated current devices that biaxially test soft tissue.

From this research and through phone interviews with suppliers and manufacturers, the project team identified the gold standard for biaxial soft tissue testing devices. The various types of available gripping mechanisms for soft tissue were also outlined through this research. Other

potential gripping mechanisms were investigated. The team researched the structure, function, and available types of force transducers. Verifying the capabilities of the current equipment is vital to the device design, and force transducers are the costliest design component. The required sensitivity of the device force transducers and load cells was then determined based on current biaxial testing studies and quantitative values of various soft tissues in deformation. A comprehensive overview of the testing and sensitivity of the current force transducers can be seen in Appendix B. After this extensive background research and multiple client interviews, the team defined the objectives, constraints, and functions of the final design.

Idea Generation and Evaluation

The team created a pairwise comparison chart to quantitatively compare the identified design objectives. Next, the team devised preliminary designs and functional blocks following the requirements and specifications determined through the client statement, the needs statement, and relevant literature. In addition, a set of design constraints was created to ensure product feasibility within given physical and financial limits. A variety of design alternatives were constructed for each design aspect and all possible approaches were considered by the team. When developing the preliminary designs, the components of current market designs were also considered. It is important to consider design ideas from all scientific aspects to ensure limiting factors have been evaluated. Each design is compared based on practicality, reliability, repeatability, cost, and speed. From the evaluation of these preliminary ideas, using the formerly developed objectives, functions, and constraints, a final design was identified. It is necessary to apply numerical values to each alternative design to define dimensions, functions, materials, and costs.

Prototyping

The prototyping of the biaxial test device consisted of various phases based on iterative design. Experimental parameters and design calculations were applied to each design, and computer-based simulations were used to evaluate the feasibility of preliminary designs. The first iteration of grip prototypes was constructed from materials at hand, such as wires or various adhesives, to test dimensions, functions, and practicality. To simulate soft tissue scaffolds, material such as rice paper and chicken skin were used as the “tissue” to biaxially test early prototypes. Each design was evaluated for advantages and disadvantages before continuing to the next prototyping phase.

The highest functioning designs, characterized using the pairwise objective chart, were selected to be modeled with Computer Aided Design (CAD) and then machined. Based on the testing of these designs for function, reliability, and repeatability, secondary plans for designs with limited feasibility were determined. The grips were tested with the debugged program and force transducers, and all designs were constructed, and parts ordered within the \$1,000 budget.

After the evaluation of these early prototypes, a final design was chosen for manufacturing. This design was verified through the testing of cardiac patches and lay user trials, and necessary changes were made based on results and conclusions. The design was validated by the client and advisor to ensure user need and requirements are met.

Financial Statement

The team is confined to a \$1000 budget when designing this device as stated by the Department of Biomedical Engineering at Worcester Polytechnic Institute. If the team was not confined to this budget, the cost of this device could increase drastically. Research was conducted to explore the possible updates that could be made to the current device. If the

transducers were updated, using the same manufacturer, Futek, it would cost a minimum of \$1200 per transducer [33]. Depending on the specifications and manufacturer of transducers, this cost could increase to \$6400 per transducer. Transducer specifications are detailed in Appendix C. In addition to new transducers, there is the option to purchase Biorakes as a grip option. The Biorakes are available in packs of four from CellScale for \$316 [23].

Additionally, through discussions with National Instruments, a source of both software and hardware incorporated into the device, a comprehensive cost estimate was generated to update the current equipment. This device and subsequent testing requires high sensitivity, increased control, and increased lifespan. Overall, updating the National Instruments technology of the device would cost an estimated \$4090, but would extend the lifespan of the device for use over the next 10 years, and would improve the data acquisition and analysis rates as well as motor control. The comprehensive quote is detailed in Appendix D.

Based on the information above, a cost analysis was completed. This device, if modified to have the most precise and up to date equipment, would cost \$6800. This cost includes an updated and compatible software and hardware system from National Instruments, increased sensitivity force transducers from Futek, and precisely manufactured rakes, using CellScale as a price reference.

4. Design Process

4.1 Needs Analysis

The need for this project was to improve Worcester Polytechnic Institute's biaxial testing system to effectively grip anisotropic soft tissue and bioengineered materials for biomedical applications. Researchers at WPI need a device to effectively grip and accurately evaluate stress-strain properties of newly developed bioengineered tissue. The currently accessible technology at the university does not sufficiently grip these soft tissues. Uniaxial testing does not accurately evaluate sub-failure characteristics of soft tissue due to the anisotropic and nonlinear stress-strain properties. The current biaxial device is programmed to test sub-failure properties, but cannot effectively grip extremely soft specimens to meet the needs of the client.

The biaxial device provides the user with reliable data to determine the functionality of soft tissue or bioengineered materials. The device needs to produce forces below 2 N, in order to capture the properties of very small specimens of extremely soft tissue. Cardiac heart patches act as a baseline for sensitivity of this device, as they consist of very few, soft layers, that each exhibit a low tensile strength. Myocardium of a healthy adult has a contractile force as low as 20-50mN/mm². When a 1 cm by 1 cm patch is tested, the force acting over this area could be as low as 2N. The patch size used in this device will range from 1 to 2.5 cm in width and length. It is important that the sensitivity of the device is low enough to produce and measure these forces.

The attachment method of the soft tissue specimen is important in facilitating accurate testing. The method of attachment or the gripping system must allow for lateral movement. Additionally, it should not affect the mechanical properties of the sample or the results of the testing. The attachment should allow for sub-failure properties to be accurately measured and should not fail at any point during testing.

The team ranked the objectives of the attachment system using a pairwise comparison chart, seen in Table 4.1. Through this comparative method, a cell with a row objective deemed more important than a column objective received a “1”. A cell corresponding to a row objective deemed less important than the column objective received a “0”. The team then summed the total of the row and ranked the objectives in order of importance, with the objective scored a “5” representing the most important.

Table 4.1: Pairwise Comparison Chart of Attachment System Objectives

	Usable	Force Distribution	Specimen Preservation	Manufacturable	Repeatable	Total
Usable	-----	0	0	1	1	2
Force Distribution	1	-----	1	1	1	4
Specimen Preservation	1	0	-----	1	1	3
Manufacturable	0	0	0	-----	0	0
Repeatable	0	0	0	1	-----	1

The main objectives of this project are to provide a method of effectively gripping and loading anisotropic specimens for biaxial testing; therefore, the related objectives, force distribution and specimen preservation, both received the highest scores of 4 and 3 respectively. Another important objective, usability, was ranked third in importance because current attachment methods for this kind of testing exist, but require extreme skill and time to attach without deforming the specimen. Following usability, repeatability was ranked fourth in

importance as the proposed gripping mechanism may be coupled with loading tool to ensure precise attachment of the specimen for a repeatable loading system. Finally, manufacturability was ranked as the least important objective as there exist many manufacturing resources for this design process. Manufacturing the proposed gripping mechanism does not pose as a considerable limitation to the final design.

Secondary constraints of the design include the compatibility of the loading system with the existing device, the biaxial test device developed by the WPI major-qualifying project team of Chong, Hung, Steinhart, and Trexler in 2005 [34]. The specifications of each component of the loading system must be within the size and geometric constraints of the existing device. The device must also be safe for the user to operate and demonstrate successful function by biaxially testing the specimen and measuring the sub-failure stress-strain properties. The final constraint limits the timeline of the project with completion scheduled for May 2018.

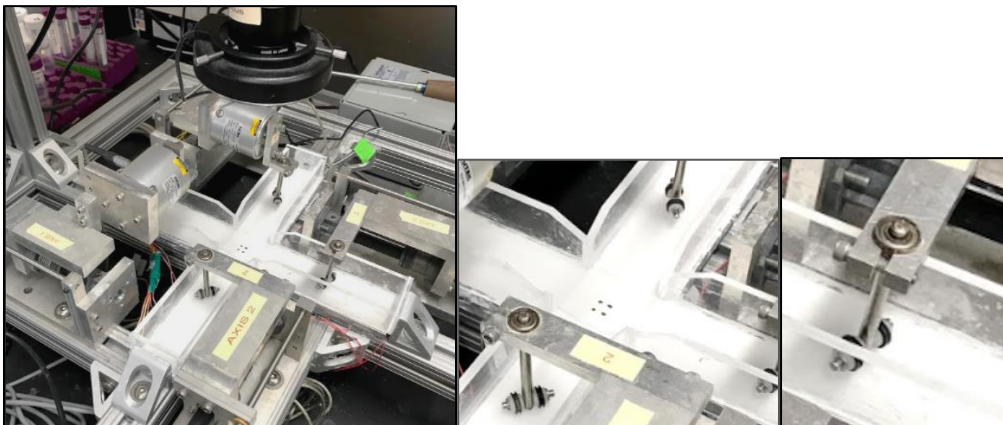


Figure 4.1: Crucial components for consideration of the current device at WPI (left). The cruciform-shaped bath (center) and the bearings (right).

4.2 Concept Maps and Designs/Prototyping/Feasibility Studies

Based on research of biaxial testing, the team developed conceptual designs to successfully test anisotropic soft tissue. These designs were developed in order to meet the

previously specified objectives of the device. These specifications include usability, repeatability, and the allowance of lateral movement and shear. Each of the conceptual designs pursued below offer various advantages and limitations.

Velcro

Research of biomimetics is growing in popularity for use in biomedical applications. Biomimetics is the imitation of the models, systems, and elements of nature for the purpose of solving seemingly unrelated problems. One example of a biomimetic design is Velcro, which is a synthetic adaptation of burrs. Velcro was originally created when George de Mestral was walking through the woods and a number of burrs stuck to his clothing. He wanted to utilize that attachment design by engineering a similar gripping mechanism of very small hooks and loops on two pieces of fabric that stick together [35]. The team hypothesized that this method may be an ideal gripping mechanism for soft tissue, with tiny compliant hooks to hold the sample in place with minimal damage to the specimen and an even distribution of forces.

The feasibility of this design was evaluated through uniaxially testing hydrated rice paper on an Instron 5544 with strips of Velcro. Two square pieces of Velcro were placed around the edges of a square sample of rice paper, 2.5 cm by 2.5 cm, overlapping about 3 mm of the sample. The opposite end of the hydrated rice paper was secured the same way with two additional squares of Velcro. The Velcro was loaded into the Instron in Goddard Lab 207 at WPI as shown in Fig. 4.2.



Figure 4.2: Uniaxial Instron test of hydrated rice paper with Velcro grips

This sample was uniaxially pulled in tension at a rate of 20 mm/min. Within the first second of testing, the hydrated rice paper slipped from the Velcro grips. This test was run three times, and each time the Velcro could not efficiently secure the sample in place. It was concluded that Velcro is not an effective gripping mechanism for soft tissue as the hooks are too shallow to both pierce the sample and secure to the other fabric strip.

Setting

The team researched the feasibility of strengthening the edges of the test specimen to minimize damage during gripping while maintaining the mechanical properties of the center of the specimen for evaluation. This additional setting of the edges to prepare for gripping may be accomplished through the application of heat, light, or chemicals. Both quick-freezing and cryogenic wave jaws have been shown to be an effective method to set the edges of a specimen. Cryogenic wave jaws are clamps which both hold the specimen in place and freeze the edges

[36]. Quick-freezing the edges of a specimen strengthens it so that it may be held by clamps, while the material properties at the center of the specimen are maintained for evaluation by biaxial testing [37].

Setting the edges of soft tissue maintains some of the material properties of the sample and has been used as a method for biaxial testing. However, it is not a feasible attachment method for this application of the biaxial test device, because the technology is expensive, and it may alter properties of these incredibly delicate and soft specimens further than the edges.

Grips

The team considered the best gripping mechanisms for soft tissue that would minimize stress concentrations and not damage the samples. To determine the most efficient gripping mechanism, the team researched, designed, and tested various attachment methods and materials using the Instron 5544 in the lab of Goddard Hall 207 and the biaxial device in Gateway Park at WPI. The following attachment methods were considered:

- Clamps
- Sutures
- Rakes

The testing performed provided an assessment of possible attachment methods for the final prototype. This section describes the testing completed and a comparison between the effectiveness of each gripping mechanism.

Clamps are often used to test soft tissue due to their ease of use and repeatability, but are known to allow very limited range of motion at the attachment site, limiting their use for biaxial soft tissue tests. The team evaluated their effectiveness by testing a specimen of hydrated rice paper in the clamps of the uniaxial Instron machine. It was observed that the rice paper proved to

be quite elastic and stretched to twice its original length, but failed at the grips. The team performed this test three times, and during each test the sample failed at the grips. This testing supported the hypothesis of considerable stress concentrations created at the grips, which limits use for the biaxial testing of very compliant soft tissue.

The team evaluated the effectiveness of sutures by performing tests on both latex gloves and rice paper samples. The sutures tested on rice paper were constructed using pieces of thread and staples. Thread was tied to each staple once secured to the specimen, and the ends of the thread on each side were commonly joined by using a piece of tape. These sutures were tested in the Instron, shown in Fig. 4.3. For uniaxial testing, the team found these sutures very difficult to use and attach to the sample, which was evident in their quick detachment during testing. It was noted that when preparing a sample to be tested biaxially with sutures, attachment of the sample to the sutures took approximately 30 mins. It took an additional 10 minutes to attach the sutures to the device. The amount of time it took to load the sample led the team to conclude that a much more effective loading system is necessary in order to maintain the integrity of samples and offer high usability.

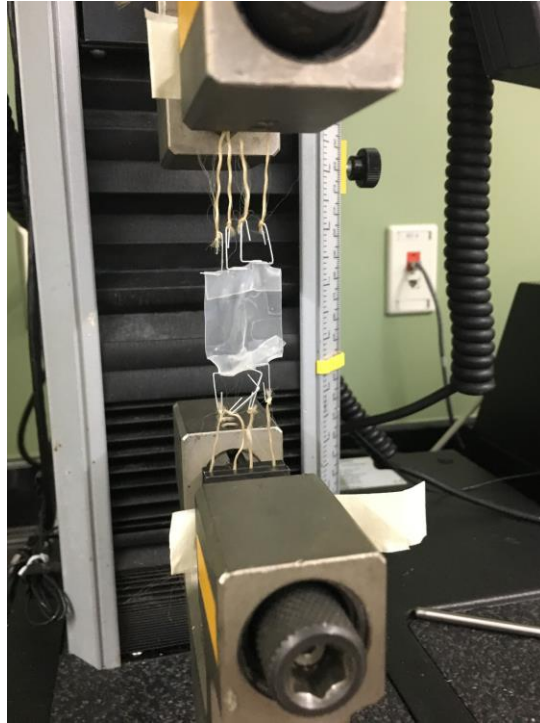


Figure 4.3: Uniaxial tensile testing of hydrated rice paper using sutures

The team assessed the effectiveness of using stainless steel rakes as grips. The material used for the rakes was 1 mm diameter stainless steel braided wire obtained from Home Depot. One rake was constructed by cutting four pieces of wire to a length of 30mm and inserting one end of each wire in between two foam pads obtained from Goddard Lab, as seen in Fig. 4.4. The opposite ends of the wire were bent to a 90-degree angle with pliers to be inserted into the specimen. Two of these rakes were constructed to be used in uniaxial testing in the Instron in Goddard, shown in Fig. 4.5. It took multiple attempts to insert the wire into the hydrated rice paper, and it proved difficult to successfully insert all four prongs of a rake at once. However, upon testing the team found the rice paper successfully failed at the middle of the sample. This shows that the stress was able to transfer from the attachment point to the center.

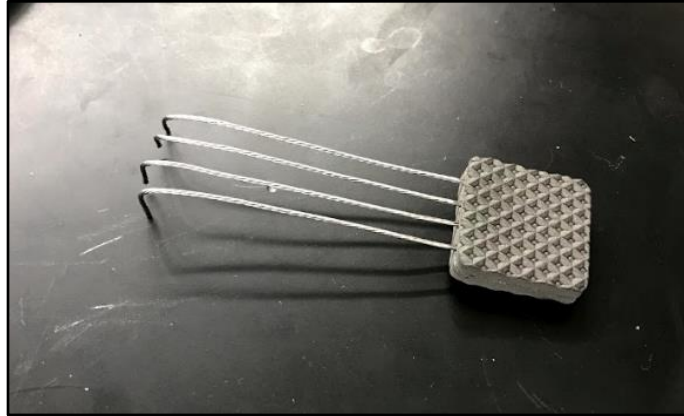


Figure 4.4: Stainless Steel Braided Wire Rake Prototype



Figure 4.5: Uniaxial test of hydrated rice paper using initial rake prototype design

After testing each method, the team concluded that rakes are the most user-friendly gripping mechanism and also perform the best during testing with low load time, satisfactory specimen preservation, and reliable attachment repeatability. The rake grips also remained attached to the sample throughout testing. The Velcro was easy to load, but ineffectively gripped the sample as the specimen detached from the Velcro early in the uniaxial test. Finally, the

loading time for the sutures was considerably longer than desired; however, the sutures did provide the most lateral movement during testing. After completion of this preliminary testing, the team determined the most effective gripping mechanism would combine a rake attachment that freely pivots at the base to incorporate the sutures' advantage of lateral movement.

4.3 Alternative Designs

After conducting feasibility studies with the aforementioned conceptual ideas, the team decided that grips were the most viable option. Taking into consideration the benefits of both sutures and rakes as gripping mechanisms led the team to identify individually pivoting rake tines with a separately pivoting base as the ideal mechanism to allow for shear and lateral movement in the specimen. The basis for this mechanism used pivots as an element to allow for lateral movement, like sutures, while incorporating rakes for repeatability and usability. Based on this mechanism, the team designed several alternative designs.

Gripping Mechanism

The first design the team generated was a stage design seen in Fig. 4.6. This design is composed of a T-shaped base of UHMWPE with four 0.5 mm diameter holes that act as pivots for the rakes. The purpose of the T-shape is to provide a supportive base underneath the thin tines during loading. The entire system can be mounted onto the existing bearings on the device using a small clamp. The holes allow for the tines to move freely in the lateral direction, allowing for lateral movement in the sample during testing. Attaching the base of the system to the bearing on the machine allows for further range of motion and for shear in the sample. This design is easy to manufacture, as the base is a simple T-shape, and is easily attachable to the existing device.

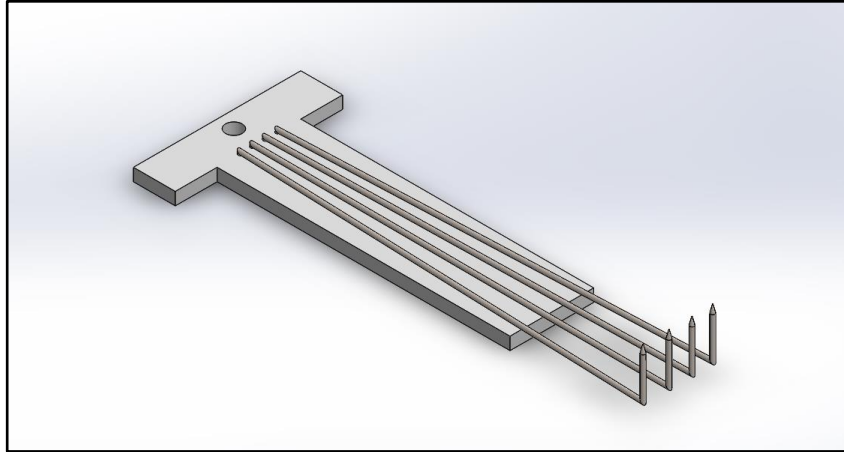


Figure 4.6: The first alternative design idea - Stage Design

Another design the team created is a system of paired pivots in order to increase the limited range of motion offered by the first design. This design uses two individual, circular pivots on a base, seen in Fig. 4.7 below, in order to achieve additional range of motion. The two circular pivots move independently of each other and the tines are able to freely pivot as well. The entire base can attach to the existing bearing on the machine. This design, while allowing for maximum range of motion, would be difficult to manufacture because of the many small parts it requires. One dimension of the individual pivots is under 5 mm in diameter, which would be difficult to manufacture. Also, because of all the moving parts, it would be more difficult for the user to handle.

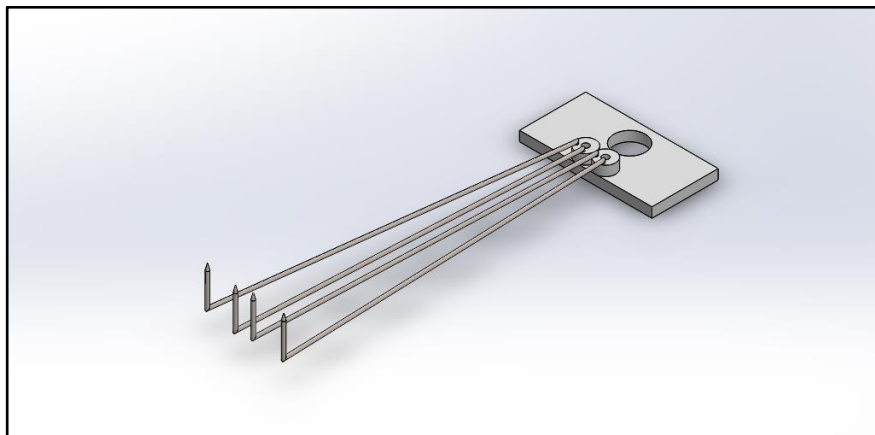


Figure 4.7: Alternative grip design - Paired pivots

Another alternative design developed was similar to the paired pivots but attached the tines to one circular base, seen in Fig. 4.8 below. This grip was designed mainly for ease of manufacturing. It is user friendly and requires very little material for the base, limiting the cost as well. However, the circle design has the lowest range of motion and will also require two different length tines in order to align correctly in the tissue.

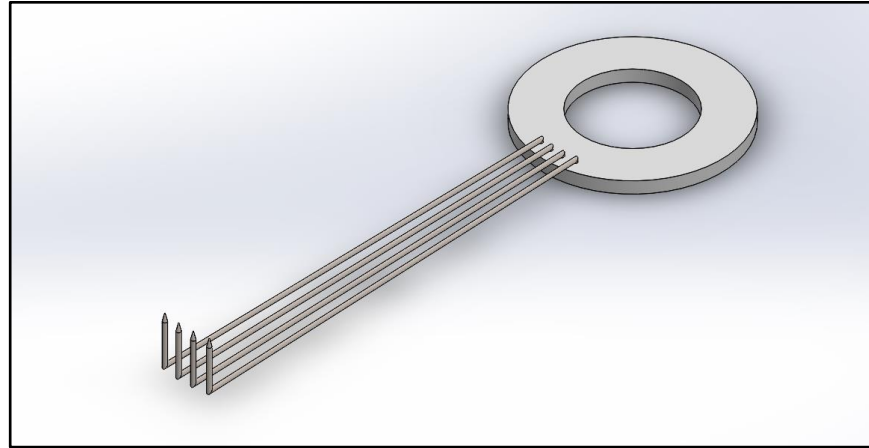


Figure 4.8: Alternative grip design - Circular base design

The final alternative design focused more on the attachment method to the existing device. This design is two separate parts that mirror each other and attach on to the bearing pole of the biaxial device, shown in Fig. 4.9. It prevents rotation of the base in all directions, providing stability. It is also user friendly because the attachment method is simple and quick. However, this design requires much more material than the others, so it is costlier. It is also difficult to manufacture due to the holes on the inside of the base for attachment.

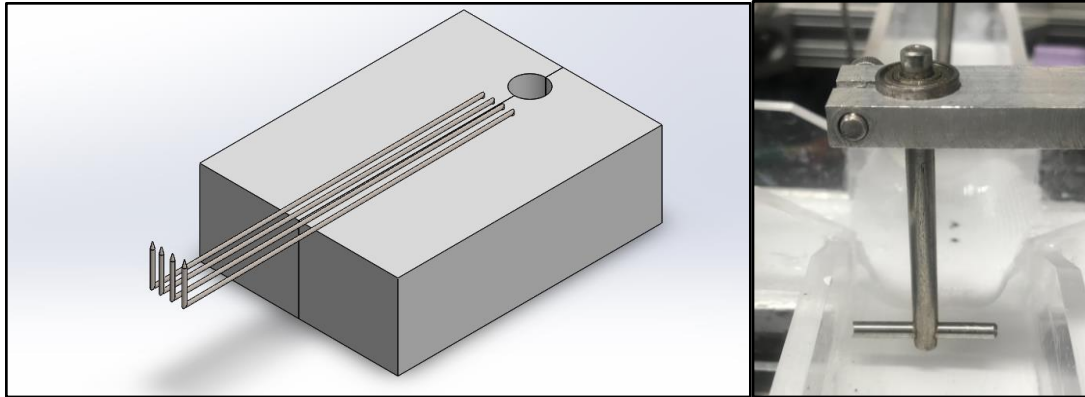


Figure 4.9: (left) Alternative grip design - Chairlift design, (right) bearing pole on existing device

Loading Mechanism

In addition to grip designs, the team also developed multiple loading mechanisms. The designs had to be compatible with all of the alternative grip designs. The main thought process of the team was to have two parts; one piece to evenly space out the tines and hold them in place during loading, and the second piece to mount the specimen onto the rakes. The team decided to rapid prototype these parts because of the intricacy of the parts, the size, and the precision required. It is also important, mainly for the spacing tool, that it be prototyped out of a material that is denser than water, so it will not float in the liquid bath

The first idea the team generated was the tine spacers, seen below in Fig. 4.10. For this, something simple was needed that could be placed over the middle of the tines to keep them equidistant apart during loading. This spacer could be used over any of the tines on the alternative grip designs because they are all the same distance apart from each other. The design would be a 1 cm square and 5 mm thick and have extruded cuts the width of the tines and spaced correctly apart on one surface, so it could simply be placed over the tines and hold them in the correct position during loading. This design is simple, requires very little material, and is easy to rapid prototype.

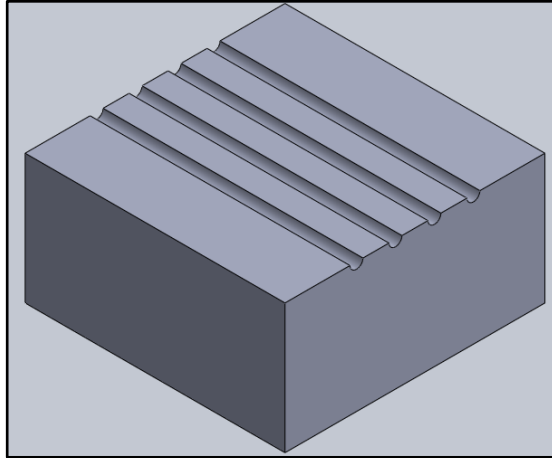


Figure 4.10: Alternative loading tool - Tine spacer

Another alternative design is for the platform loading tool. The team came up with a “sandwich” mechanism, seen below in Fig. 4.11, that would be two 2.5 cm square pieces, each with four 0.5 mm cuts going into 0.5 cm from the center on every side. These slits would be able to be placed over the tines after being separated by the spacer tool. The idea with this loading tool is to puncture the specimen, of dimensions between 1.5 cm and 2.5 cm, through the cuts in both pieces by simply lowering the assembly onto the rakes. The bottom piece would ideally fall away after loading is complete and the top piece could be taken off manually. This design is easy to manufacture using rapid prototyping and is simple to use.

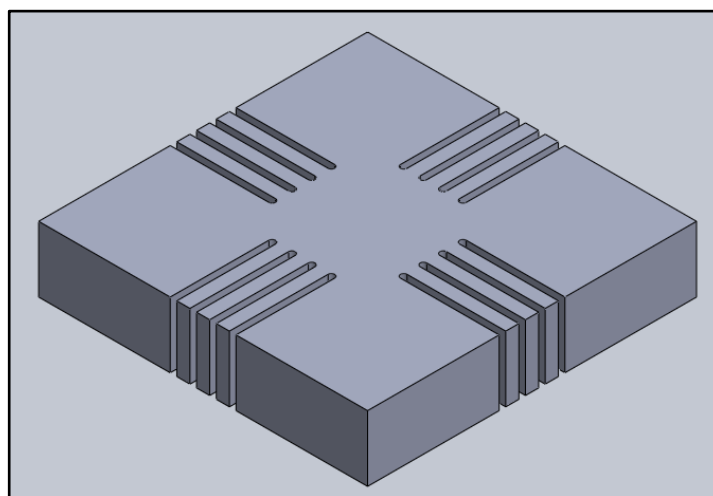


Figure 4.11: Alternative loading tool design - Platform tool

Another loading tool the team came up with is a stamp method. This method would use a handle and loading area for the specimen to stick to, then the user would, after spacing the tines out with the spacing tool, press the specimen onto the rakes. The loading area would be made of a spongy material that would allow the rakes to puncture through. This method is simple to use but could induce harm to the sample if not handled gently, because the stamp must be peeled off of the specimen after loading.

Finally, the team developed an alternative design that works like a stapler. This design would consist of two parts, like the platform tool, with notches in the bottom piece to be placed under the rakes for alignment. The top part has holes through which the tines will puncture, and the user would simply stick the specimen to the top piece and press the bottom and top pieces together to puncture the specimen. This method would most likely be the most difficult to manufacture and use and would require multiple top pieces with differently spaced holes in order to accommodate a wide range of specimen sizes.

4.4 Final Design Selection

Gripping Mechanism

Through qualitative comparisons, the team evaluated the achievement of the identified objectives by each potential grip design, detailed in the previous section. This evaluation was completed through a weighted comparison matrix. Each design objective was assigned an objective weight, from 1 to 5, based on its importance to the effectiveness of the design. An objective assigned a weight of 5 represents an objective with the highest importance. The proposed designs were then scored a rank, 1 through 4, representative of the design's ability to achieve that objective in relation to the other designs. The weighted total of each design was then calculated using the following equation, with i representing each of the 5 objectives:

$$\text{weighted total} = \sum (\text{design rank})_i * (\text{objective weight})_i$$

The resulting comparison matrix is shown below in Table 4.2.

Table 4.2: Weighted Grip Design Comparison Matrix

Objective	Specimen Preservation	Force Distribution	Usability	Repeatability	Manufacturability	Weighted Total
Objective Weight	5	4	3	2	1	--
Design						
Stage	4	2	3	4	4	49
Paired Pivots	2	4	1	1	1	32
Circle	1	1	4	2	3	28
Chair Lift	3	3	3	2	2	42

Based on this weighted comparison matrix, the team determined the Stage grip design to be the most effective in achieving the identified grip design objectives. After finalizing the grip design, the student researchers proceeded to manufacture preliminary prototypes. For cost efficiency and device compatibility, ideal design dimensions were identified, and a scaled prototype was created in SolidWorks.

The two main components of the final design include four rake tines, bent at opposing 90-degree angles on each end, and a stage base to support those tines and allow for lateral movement through free pivots. First, the rake tine dimensions were considered. To allow maximum shear in the sample while maintaining attachment through the duration of testing, the tines must be sharpened to a point to precisely puncture the specimen at the attachment points, while minimizing surrounding sample damage. Additionally, the tines must be thin to create those small attachment points; however, these tines must remain erect during loading and testing of a sample and must withstand bending forces in all directions. To ensure lateral movement, the tines will freely pivot on one end to allow for shear within the sample, characteristic of anisotropic specimens. Lastly, the tines must also resist wear, degradation, or rusting when submerged in solutions of PBS media used within the bath of the device to hydrate the samples to simulate *in vivo* conditions.

Considering each of these tine-specific objectives, the team identified stainless steel as an ideal tine material. Stainless steel is a rigid, rust-resistant metal that can be manipulated to hold a specific shape. Stainless steel is also available in the form of quilter's pins with a 0.5 mm diameter and pre-sharpened end.

The second design element is the base. The stage is designed with four precise holes puncturing the thickness of the stage to act as free pivots for the tines. It also includes a larger hole to serve as a device-compatible attachment location for the grip to the inverted T-bar currently on the device. The stage also must be small and lightweight to minimize any additional weight on the motors and force transducers during testing. Because the stage design is intended to support the rake tines from bending under gravitational forces, the tines interface with the stage material along their full length.

To ensure manufacturability, maximum lateral movement, and minimal friction, the team determined manufacturable and cost-efficient materials to use for the stage element. Low friction materials identified were ultra-high molecular weight polyethylene (UHMWPE) and polytetrafluoroethylene (PTFE), also known as Teflon. UHMWPE interfaces with stainless steel at a low friction coefficient of 0.18, while Teflon interfaces with stainless steel at a coefficient of friction of 0.04. However, upon further research, the team chose UHMWPE due to availability, cost, and manufacturability. Teflon was harder to obtain, more expensive, and harder to fix during manufacturing due to its extremely low friction surface.

The team first manufactured a large-scale prototype using stainless steel rod of 1.5 mm diameter, obtained from Washburn Machine Shops at WPI, and UHMWPE of 0.95 cm thickness, obtained through Amazon.com. The manufacturing of this prototype was done manually, using wire cutters, a press, and grinding wheel and drill to shape the tines, and saw and drill to create

the stage base. This large prototype, shown in Fig. 4.12, helped the team to identify necessary revisions to the design and highlighted the variability of production from manual manufacturing.



Figure 4.12: First prototype of the final grip design produced on a large scale. The tines are 1.5mm diameter stainless steel mounted in a 0.95 cm thickness base of UHMWPE

The team repeated the manual manufacturing of the final design using smaller dimensions. Quilter's pins 0.6 mm in diameter, from A.C. Moore, were obtained for the tines and the same stage base material was used. The pins came pre-sharpened, eliminating the need for manual sharpening and minimizing the variability in production of the tine points. However, the team identified the need for a tool to precisely bend the tines to the opposing 90 degrees on each end. The smaller prototype, shown in Fig. 4.13, supported the team's previous conclusion that manual manufacturing was too variable to produce the necessary quality of the final grip design.

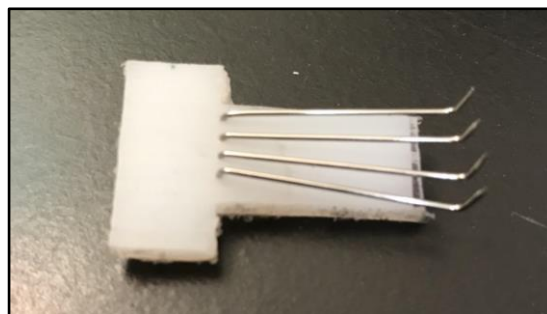


Figure 4.13: Second prototype of the final grip design produced on a smaller scale. The tines are 0.6mm diameter stainless steel mounted in a 0.95 cm thickness base of UHMWPE

The third prototype was produced using fine quilter's pins, measuring 0.5 mm in diameter and the same base material. To increase the precision of the stage base, the team used a programmable mill in Washburn Machine Shops at WPI. The stage design was translated from a

SolidWorks part to an Esprit model. This program was then uploaded on to the Haas VM2 programmable mill. Using a vacuum plate, the team secured the base to the machine and precisely machined the stage base following the Esprit program model, leaving 0.02 cm thickness of the base material intact during the cut to maintain the vacuum seal. The pieces were then removed from the UHMWPE sheet using an exacto knife. The produced stage set was considerably cleaner and more precise than the manually manufactured bases. However, the team felt that due to the small scale of the design, further precision was necessary to produce a repeatable, usable gripping system.

The final iteration of the grip design utilized 3D printing to maximize cost efficiency and precision. After careful consideration of the space available in the device and the size of the specimens to be tested, the team shortened the stage to allow for enough room to test all specimen sizes. Further, a hole was placed at the end of the stage to allow for easy attachment to the current device, utilizing the existing bearing-shaft mechanism. The stage was manufactured from low-friction Nylon in the MarkForged Mark Two 3D printer and is shown below in Fig. 4.14.

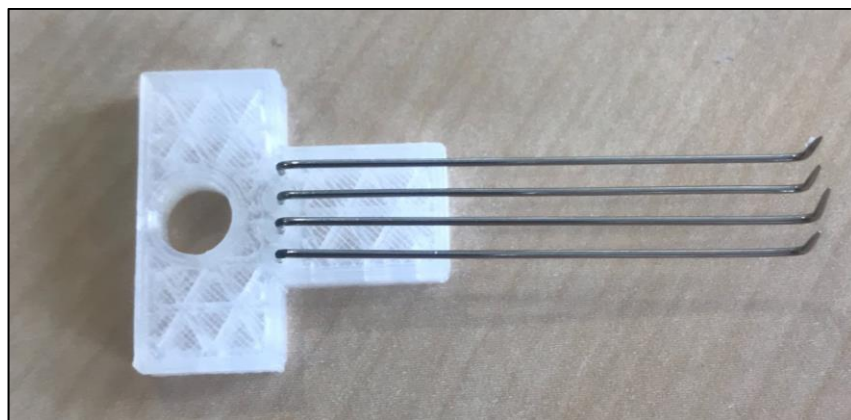


Figure 4.14: : Final grip design using a 3D printed stage of low-friction nylon with four stainless steel quilter's pin tines

Loading Tools

After selecting the final gripping mechanism, the team qualitatively compared each loading tool. The criteria for this comparison was based on the objectives previously explained. Similarly, to the gripping mechanism, each design was then evaluated based on how well each objective was met. This evaluation was completed through a weighted comparison matrix. Each design objective was assigned an objective weight, from 1 to 5, based on its importance to the effectiveness of the design. An objective assigned a weight of 5 represents an objective with the highest importance. The proposed designs were then scored a rank, 1 through 4, representative of the design’s ability to achieve that objective in relation to the other designs. The weighted total of each design was then calculated using the following equation, with i representing each of the 5 objectives:

$$\text{weighted total} = \sum (\text{design rank})_i * (\text{objective weight})_i$$

The resulting comparison matrix is shown below in Table 4.3.

Table 4.3: Weighted Loading Mechanism Design Comparison Matrix

Objective	Specimen Preservation	Grip Compatibility	Usability	Manufacturability	Repeatability	Weighted Total
Objective weight	5	4	3	2	1	--
Design						
Tine spacers	4	4	4	3	4	58
Specimen sandwich	3	3	1	4	3	41
Stamp	2	2	2	2	2	30
Stapler	1	1	3	1	1	21

The objectives of the loading mechanism were changed to better represent the goal of the tool. Our final loading tool must be compatible with the grips, as they will work as a system to facilitate easy specimen loading. Based on the weighted matrix, the team determined that the Tine Spacers and the Specimen Sandwich would be the most effective in achieving the objectives. The team realized that the Tine Spacers alone would not fully accomplish the goal

and utilizing two design mechanisms would be the most effective. Once the final design was chosen, the team could begin to prototype the designs.

Each design was modeled using SolidWorks, iterating the optimal dimensions and geometry. The simplicity and precision of each design, led the team to choose 3D printing as the rapid prototyping method. Worcester Polytechnic Institute has four options for 3D printers, each with different capabilities and material options. One consideration for the loading tooling was to use a low friction material for the tool interacting with the specimen, as minimal friction enhances specimen preservation. The material had the biggest influence on the machine chosen. Each machine was researched to learn about the capabilities and material options. Based on this research, the team learned that due to the simple geometry and size of the design, all four of the 3D printers owned by WPI could adequately print the prototype. The best choice for the loading tools was the Markforged Mark Two, due to the material options. The material this printer uses is nylon, which is a low friction material. Additionally, this material is durable and will not be affected by the PBS solution used during testing.

Rapid prototyping allowed the team to make multiple prototypes as changes were made from testing. It was a low cost, repeatable way to manufacture both the Tine Spacers and Load Platform. The loading tools were optimized through various testing to determine the best size and shape to be compatible with the grips, specimen, and the user. The first iteration of the prototype can be seen in Fig. 4.15.



Figure 4.15: First prototype of tine spacers and loading platform

After testing using the first iterations of the loading tools, the team noticed some problems with the design. The indentations on the tine spacers were too shallow, not allowing adequate depth to grip the tines to hold them in place. Additionally, the parts were very small, making them difficult to handle.

The second iteration of the loading tools was intended to maximize usability. The loading area within the bath walls of the device is extremely small, making it difficult to maneuver the load platform within the confined area. To facilitate the use of the tine spacers, the team made each spacer taller, to serve as a handle for easier gripping, seen in Fig. 4.16. In the loading platform, both pieces were redesigned to incorporate vertical handles so that a user can easily lower a specimen into the bath, utilizing the free space above the device rather than the restricted area within the bath walls. The team also included two pegs on the bottom piece of the load platform that align with two notches within the top piece to ensure proper alignment of the whole assembly during use.

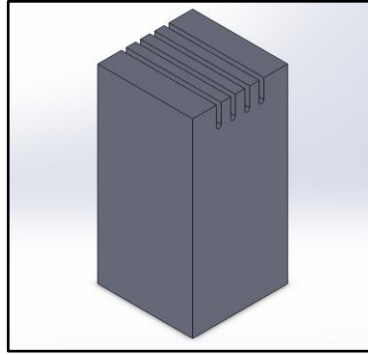


Figure 4.16: Second iteration of tine spacers

After additional testing, the team noticed that while the tine spacers kept the tines in place, it did not minimize movement of the grip from the bearing. The final iteration of the tine spacers altered the dimensions of the spacer so that each unit sits on top of the tines and supporting stage of the grips, then spans the width of the bath so that the grips are unable to pivot while the user is loading the specimen. The long handle and the alignment pegs of the load platform were shortened to facilitate the removal of the bottom piece by sliding it out from under the specimen and grips. This final iteration is shown below in Fig. 4.17 as an assembly of all of the parts.

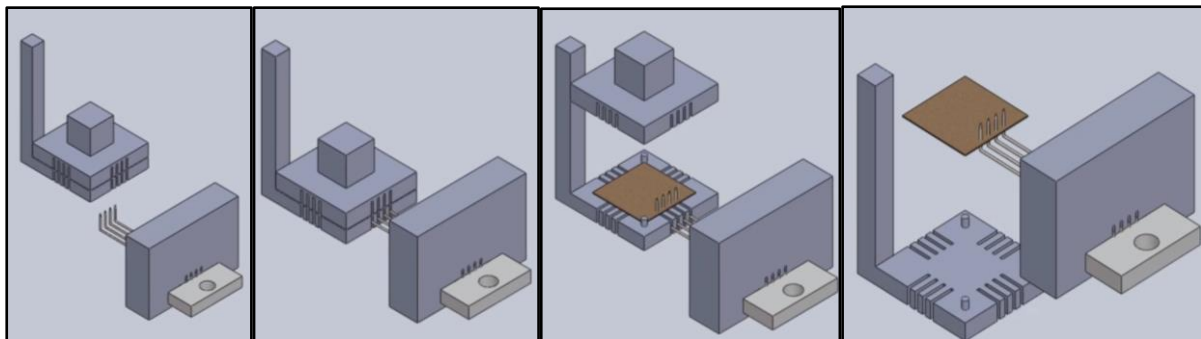


Figure 4.17: Final iteration of loading tools including both tine spacers and load platform (Shown from left to right, the load platform is lowered onto the tines, aligned by the tine spacer. The top piece of the platform is lifted by the handle, and the bottom piece is removed from the long handle, leaving the specimen mount on the rake tines).

The team created three sets of these loading tools for use with varying specimen dimensions. The average specimen dimensions within the range of the system, 1.75 cm x 1.75 cm, was the base dimension for the load tools. For a smaller specimen, 1 cm x 1 cm, or larger specimen, 2.5 cm x

2.5 cm, the loading tools incorporate angled grooves to align the rake tines to pierce a specimen of those dimensions. These alternative dimension tools are shown below in Fig. 4.18.

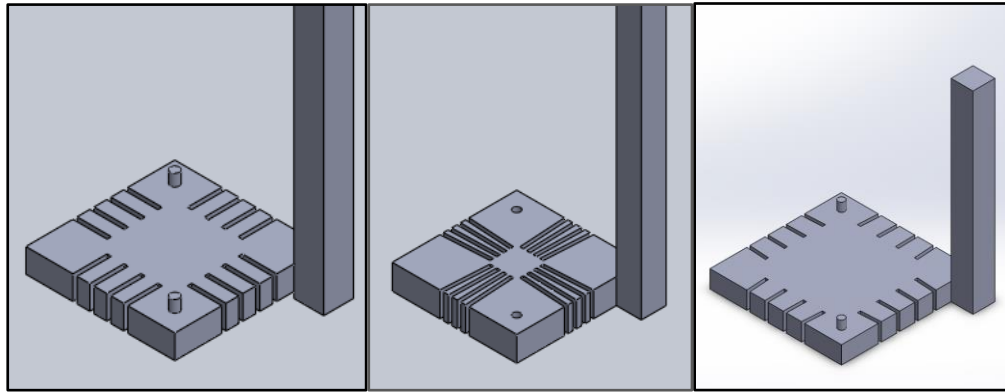


Figure 4.18: Varying dimensions for tine spacers and load platform to incorporate a range of specimens (Represented on the left is a medium sized load platform spaced for a 1.75 cm x 1.75 cm sample, in the middle is a load platform for a smaller 1 cm x 1 cm sample with angled grooves, and on the right for a large sample of 2.5 cm x 2.5 cm with angled grooves).

5. Final Design Verification

The final design of the complete attachment method was evaluated for achievement of the objectives of force distribution: shear allowance and lateral movement, and usability. The performance of the gripping system was verified through several evaluation methods that are detailed in this section, and the results were compared to accepted attachment methods, including the gold standard suture/pulley system, and the currently available BioRakes offered by CellScale.

5.1 Shear Evaluation

Allowing shear is necessary to evaluate anisotropic properties of soft tissue specimens. To evaluate the shear allowance of the final grip design, the team conducted biaxial tensile tests using square specimens, measuring 3.5 cm x 3.5 cm, of anisotropic gauze. Three specimens each were prepared with the more prominent fibers aligned along the X axis of the device, and with the fibers angled 45 degrees from the X axis. All specimens were marked with four dots in an exact square of 1 cm x 1 cm. They were then loaded onto the rakes and the force transducers were zeroed. The aperture and zoom of the overhead camera was adjusted to capture all four markers. Then, a tensile test moving all four axes in a stepwise fashion at a rate of 200 rpm was conducted until specimen failure. At each step, the force in X, in N, and the force in Y, in N, was recorded. A video continuously captured the displacement of the dots during the test.

Force-displacement of each sample was calculated after measuring the distances between the marks and finding the average length of the specimen's side in both the X and Y direction. The force-displacement curves were generated by plotting the recorded force in newtons in X and Y against the average X length and average Y length of each sample, respectively. The

force-displacement curves for the averages of three samples of gauze tested with fibers angled along the x axis are shown in Fig. 5.1. The force-displacement curves for the averages of three samples of gauze tested with fibers angled 45 degrees from the x axis are shown in Fig. 5.2.

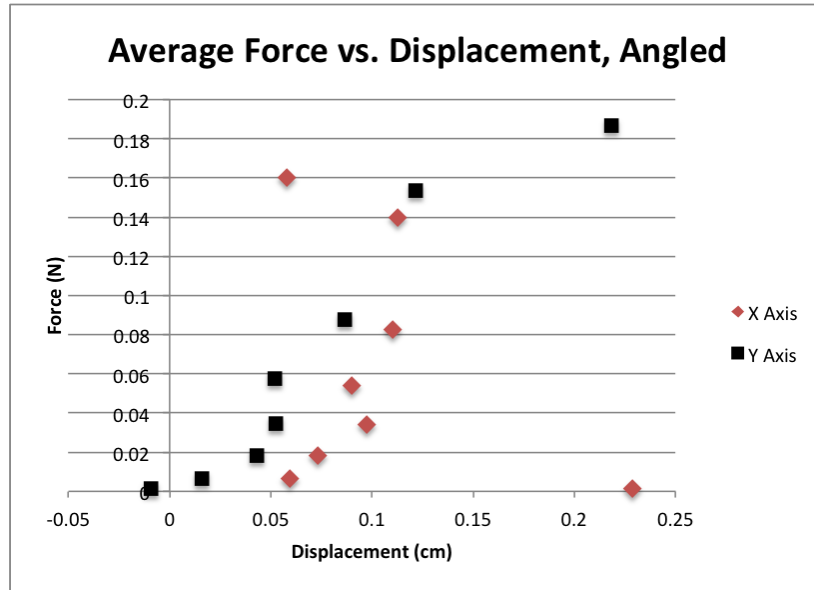


Figure 5.1: Force-displacement curves for biaxial testing of anisotropic gauze with fibers angled 45 degrees from the X axis

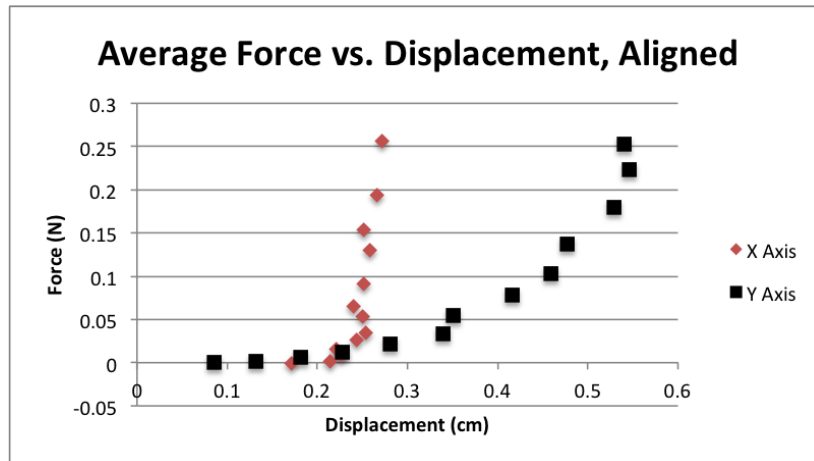


Figure 5.2: Average force-displacement curves for biaxial testing of anisotropic gauze with fibers aligned along the X axis

As seen in these graphs, it is evident that the samples are experiencing different mechanical properties on each axis due to the differences in the data series between the x and y force-displacement.

The amount of shear allowed with pivoting tines versus fixed rakes was compared. Rakes with a fixed base, to represent CellScale's BioRakes, were tested first with a sample of anisotropic gauze. The gauze also was marked with four dots in a square of 1 cm x 1 cm. The gauze was then loaded into the device to have its fibers angled at 45 degrees from the X axis. Images from this testing can be seen in Fig. 5.3. As seen in these images, the dots closely maintain the square shape and the specimen deforms uniformly despite the varying fibers, demonstrating how fixed rakes minimize the amount of shear that can be induced in the sample.

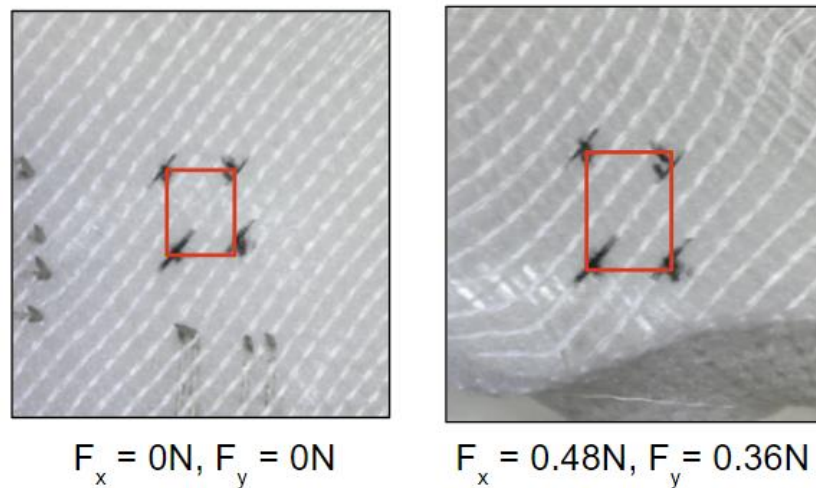


Figure 5.3: Anisotropic gauze before testing (left) and after testing (right) with fixed rakes

We then compared these rakes to our design, which has pivoting mechanisms. Another sample of gauze was marked with a 1 cm x 1 cm square and loaded into the device with fibers angled at 45 degrees to the X axis. As seen in Fig. 5.4, the square changes from a square to a rhombus after testing. The pivoting rakes allow shear to be induced in the sample. These tests were repeated over three samples to verify the results.

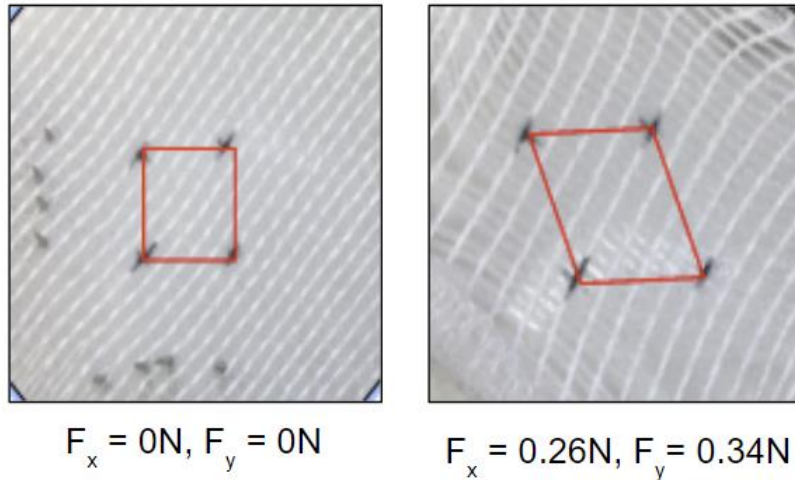


Figure 5.4: Anisotropic gauze before testing (left) and after testing (right) with pivoting rakes.

5.2 Lateral Movement Evaluation

Allowing lateral movement of the tines is necessary for an anisotropic specimen to accurately deform when biaxially tested. To evaluate the lateral movement of our design, we compared our tines to CellScale’s BioRakes. To calculate the force needed to bend a BioRake’s 30 mm long tines, we used bending calculations for a cantilevered rod of stainless steel about its end, shown below.

$$P = (3EI\Delta_{max}) / L^3$$

$$I = 0.78r^4$$

In this equation, P represents the force, E is modulus of elasticity, I is moment of inertia, Δ_{max} represents maximum deflection, L represents length, and r represents radius. The maximum deflection of the tines is 21 mm, the distance to rotate from the center of the bath to reach its walls. The force required to reach this deflection was calculated for each diameter of available BioRakes, 0.25 mm and 0.3 mm. The team also calculated the force required to reach the same deflection for a fixed tine of 0.5 mm diameter for comparison to our design. These calculations are shown below in Table 5.1.

Table 5.1: Bending Calculations of a Fixed Tine

Variable	units	BioRake 1	BioRake 2	BioRake 3
r	mm	0.125	0.150	0.250
L	mm	30	30	30
E	MPa	190000	190000	190000
I	mm ⁴	0.000190	0.000395	0.00305
Δ_{\max}	mm	21	21	21
P	N	0.0844	0.175	1.35

These calculations were then verified using a 20 oz-in Futek TFF400 rotary force transducer. A 0.5 mm stainless steel tine was fixed on one end by a clamp. The free end was then deflected 21 mm using the arm of the rotary transducer, and the corresponding average force required was measured to be 1.50 N. Then the transducer was used to measure the force required to pivot the 0.5 mm diameter tines within the stage of the grips to the same deflection of 21 mm. The two tests are shown in the schematic below in Fig. 5.5.

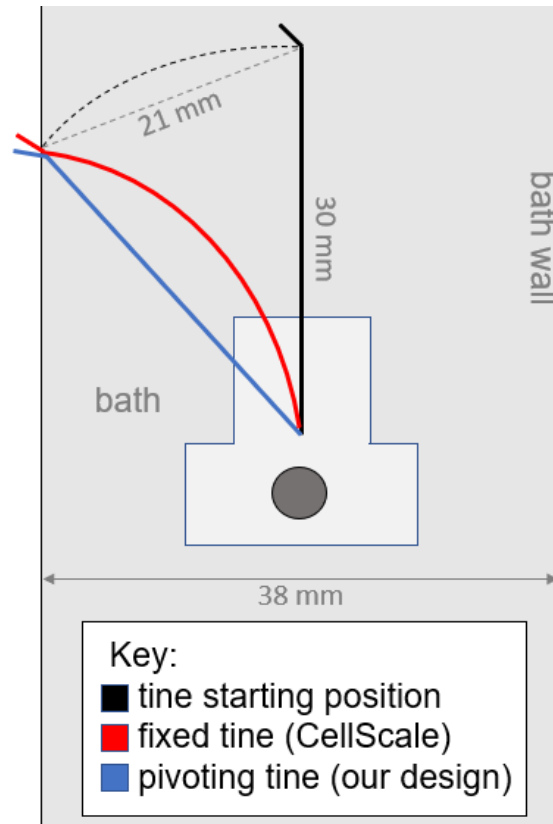


Figure 5.5: Lateral Movement Evaluation Schematic

The average force required to deflect the pivoting tines was less than the resolution of the transducer, 0.001 N. Overall, the pivoting rake tines in our device surpass CellScale’s thinnest rake, 0.25 mm in diameter, in terms of lateral movement due to decreased bending stiffness. Our tine requires a significantly smaller force to deflect to the walls of the bath reaching full range of motion than any of CellScale’s available BioRakes.

5.3 Usability

Usability was continuously evaluated through testing of the whole gripping system, including the use of the loading tools, as well as grips themselves. To ensure the compatibility of each component with the other components, assemblies were created in SolidWorks, Fig. 5.6. These assemblies allowed the team to ensure the dimensions and geometries of each piece aligned with all other components. Although these assemblies did not utilize the actual

components, it provided insight as to the compatibility and function of the components as a system. After it was confirmed that each component was compatible and usable with the other components, they were all sent for 3D printing.

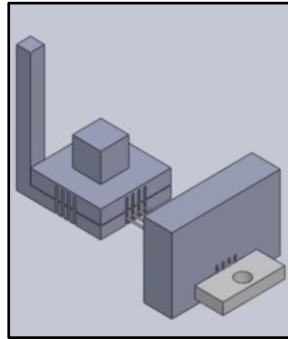


Figure 5.6: : Preliminary usability trial with all components of the system aligned

Design improvements were identified through the use of the loading tools and grips during testing of gauze samples. These identified design improvements included the incorporation of vertical handles on each piece of the load platform, as well as all tine spacers, the widening of the tine spacers to prevent the grips from pivoting during loading, and the inclusion of alignment pegs within the load platform. The final design of the entire system was used to load an anisotropic gauze specimen onto the grips. The process was timed, and the average load time to use this gripping system was less than 1 minute. The utilization of the loading system was repeated three times to verify usability.

6. Final Design Validation

6.1 Feedback on Final Design

Throughout the design process, the team gathered feedback from testing and using the components of system. This feedback allowed the team to make the necessary iterations to reach the final design. Most of the feedback came from the team and project advisor and was based on the limitations of the current device. The project advisor and project mentor provided useful feedback for each iteration that would facilitate ease of use. The main concern with the designs of the loading system was the size of components. The dimensions needed to be small enough to fit within the constraints of the bath, but large enough that the loading system was easy to handle by the user. It was recommended that a handle be placed on both pieces of the loading platform to facilitate usability. Additionally, the project advisor recommended using the narrow bath to our advantage rather than a limitation. The tine spacers were redesigned to incorporate the width of the bath to fix the grips during loading. The last recommendations were to develop additional components for the loading system to aid in alignment of the entire attachment system and to develop this system for small, medium, and large sample sizes. The recommendations and feedback received from the project advisor and project mentor helped the team to realize and manufacture the final design.

6.2 Economics and Manufacturability

The final design of this project was entirely 3D printed, making the fabrication process very repeatable and cost effective. However, the final design was made to be specifically compatible with the current device at WPI. This project was able to successfully produce a product that is economically affordable. If this design were to be used in industry, adjustments

would need to be made to the design to fit the industry device or adjustments would be made to the device to allow the system to properly attach.

The final design was made from nylon and stainless steel, both of which are inexpensive materials and readily available. The use of 3D printing for the fabrication of the design allows for very quick and precise production. Currently, biaxial test devices are sold as entire units and attachment and loading systems are not commonly sold independently. CellScale does offer their Biorakes for individual sale, which are priced at \$316 for a set of four [23]. The gripping system developed during this project could be available at a much lower cost, due to the simplicity and low cost of manufacture. Further, the concerns regarding the precision of rake tines that the team had during the manufacturing process would not apply in a large-scale production of the design. At a large scale, the rake tines could be effectively and repeatedly produced.

The downside in using additive manufacturing methods to produce the design is that any iterations of the design now become waste as they can't be reused. However, little waste is created from the actual manufacturing process as a piece is built up, not cut out. The only waste from the actual process comes from any support material needed. As the designs in this project are very simple, the support material is minimal. It can be seen that there are both positive and negatives to this manufacturing process. Overall, the team felt that the benefits of additive manufacturing outweighed the downsides.

Lastly, the design of this system is very simple allowing for easy manufacture in any setting. The simplicity of the device also allows easy changes to be made to the dimensions to best suit the intended test device. Overall, the attachment and loading system is economically efficient with high manufacturability.

6.3 Environmental Impact

The intended use of this system is to provide a repeatable attachment method for as long as possible. There should be little environmental impact and no waste from the system. If for some reason the system needs to be replaced after sufficient use, the materials used will have no harmful effects on the environment. Stainless steel is a common material often used and recycled. Further, nylon can typically be recycled through various programs. The device does not require sterilization or advanced packaging, creating no waste from the distribution of the product. Overall, this device should not negatively impact the environment from the recyclable products and limited waste.

6.4 Societal and Political Concerns

Overall, this project does not have any societal concerns. The use of the product is intended for laboratory research. The only concern that may arise is what this system is being used to test. For example, the device could have an impact on society if the tissue being tested is an animal-derived material that threatens animal rights. Further, this device could be used to test and provide data on life saving tissue, having a positive impact on society. However, both of these concerns do not directly pertain to the device and are therefore unlikely to have an impact.

Further, there would be negligible political concerns due to the use of this device in lab. This system has no intended use on humans or animals and will not require the involvement of any government organization. Additionally, this device is for scientific purposes and relatively low-controversial use resulting in little political concern.

6.5 Ethical Concerns

This system has little ethical concerns. The use of this device is restricted to in lab research and will have no impact with anyone outside the lab. The attachment system is removable from the device, but does not have any harmful effects. Further, the entire biaxially device is stationary and presents no concern for the user. The samples being tested with the device are intended to be tested for sub-failure and failure properties, therefore showing that damage to the specimen is intentional. A positive attribute of the design is the low cost. This allows users with low budgets to access a biaxial test device capable of performing to the same quality as much more costly devices.

6.6 Health and Safety Issues

The system was designed to be safely used by all users, without the need for prior training. Each component of the system is made from non-toxic materials. Some caution does need to be taken when handling the attachment system due to the sharp tips at the end of the rakes. These rake tines were produced from stainless steel quilting needles to ensure they are safe for use. This material will present no health concerns to the common user. All other components of this system do not have sharp pieces and the material is not a health or safety concern.

6.7 Sustainability

The final design incorporates components meant for long-term use. The reusable nature of the system plays an important role in the sustainability of the device. Further, the design incorporates recyclable materials. The attachment and loading system is a relatively low-cost device and is intended for a one-time purchase. The device itself is not directly related to renewable energy, but the manufacturing process is a low power, low cost process. This process

can be powered through renewable energy and ideally, would only need to be executed once for each system.

7. Discussion

To evaluate if the grip system met the objectives of usability and shear allowance (force distribution), tests were conducted to biaxially deform a sample of anisotropic gauze. This testing was repeated with samples of rice paper and cardiac patches to validate the findings. To evaluate if the objective of lateral movement (force distribution) was met, calculations of bending stiffness were performed and validated. The results of each of these tests were compared to the current gold standard for biaxial test grips. The gripping and loading system designed for this biaxial test device successfully met our objectives of allowing shear, lateral movement, and offering high usability. The following section reflects upon the findings of testing and the extent to which the objectives were met.

7.1 Shear Evaluation

The gripping mechanism the team designed proved to successfully induce shear in the samples when biaxially tested. The squares marked on the samples of gauze tested with our pivoting tines changed from a square to a rhombus after testing in every sample. This shape change demonstrates that shear was induced in the sample. When similar samples of gauze were tested with fixed rakes, the squares marked on the samples deformed uniformly and maintained their original shape. The fixed rakes minimized the amount of shear that could be induced in the sample. The effect of shear in the sample when tested with pivoting rake tines can be compared to the effects produced by sutures. The team compared the gripping mechanism to sutures when evaluating shear as it was established that sutures are the gold standard for inducing shear. The comparison of the two gripping methods showed that the developed rake tines are equivalent to sutures in producing shear in the specimen.

7.2 Lateral movement

The final design for the gripping system maximized lateral movement by minimizing bending stiffness through the individually pivoting tines. In comparison to CellScale's marketed BioRakes, this design surpassed all available sizes of BioRakes in terms of lateral movement. A BioRake of the same diameter as our design, 0.5 mm, would require 1.35 N of force to reach full range of motion within the bath walls, whereas our rakes require less than 0.001 N. CellScale's thinnest rakes, 0.25 mm in diameter, still require up to 0.084 N of force to reach full range of motion. These calculations can be seen detailed in Appendix E. From these results, it is appropriate to say that it takes negligible force to produce lateral movement in the developed rake tines. However, even CellScale's smallest rakes require a force approximately equivalent to two nickels. Due to the delicate nature of sutures, they cannot be tested for a measurable force during bending. From this experiment, it is clear that the developed rake tines and sutures have negligible bending stiffness, allowing for maximum lateral movement. The design produced by the team, therefore, meets the gold standard of sutures and surpasses CellScale's BioRakes.

7.3 Usability

The overall system increased usability of the device by offering a gripping method for soft, anisotropic material in a biaxial test. Through the use of the loading tools, including the tine spacers and load platform, the team shortened the loading time for each specimen to under 1 minute. CellScale experts require up to 5 minutes to load one specimen into a suture/pulley system on their device, creating opportunities for damage to the specimen due to prolonged manipulation of the specimen. Our design surpasses the load time of suture/pulley systems and meets the usability of BioRakes.

8. Conclusions and Recommendations

In conclusion, our combined gripping and loading mechanism meets the objectives of the project in terms of usability, shear, and lateral movement allowance. Current gripping mechanisms on the market for the biaxial testing of soft tissue do not overcome all three of the previously stated limitations. These grips include clamps, rakes, and suture/pulley systems. Our design includes individually pivoting rake tines to incorporate shear and lateral movement, surpassing CellScale's BioRakes. Additionally, our design surpasses suture/pulley systems in terms of usability.

To test our grip design, we compared our prototypes to BioRakes and suture/pulley systems. Shear was induced in the tested sample when using our pivoting rake design. Comparatively, shear was shown to be limited when tested with fixed rakes. The lateral movement of our tines outperforms that of CellScale's BioRakes, which was determined through bending calculations and validated by deflecting our tines with our force transducers. The team's design required significantly less force to deflect against the wall of the bath, making it comparable to sutures.

In terms of usability of our design, users can load a specimen with our design in a fraction of the time it takes a professional to load a device with sutures. The gripping and loading mechanism designed exceeds sutures and is comparable to rakes in terms of usability.

In the future, the team would recommend designing the gripping and loading mechanism to be compatible with other biaxial test devices. This project was specific to one device, but it could be beneficial to universalize this design be usable in different equipment. Furthermore, because the scale of these tools is in millimeters, ensuring an extremely precise method of manufacturing the tines is crucial. Machining or 3D printing the metal tines to ensure equivalent

angles of bending is recommended to improve usability. Lastly, the team recommends incorporating 4 circular wells spanning the thickness of the top piece of the load platform, arranged in a perfect square in the center. These wells serve as exact guides to mark the specimen for displacement tracking prior to loading.

References

- [1] J. Bursa and M. Zemanek, "Evaluation of biaxial tension tests of soft tissues," *Stud. Health Technol. Inform.*, vol. 133, pp. 45-55, 2008.
- [2] Will Goth, J. Lesicko, M.S. Sacks, and J.W. Tunnell, "Optical-Based Analysis of Soft Tissue Structures," *US National Library of Medicine*, vol. 18, pp. 357-385, 2016.
- [3] M. Griffin, Y. Premakumar, A. Seifalian, P.E. Butler, and M. Szarko, "Biomechanical Characterization of Human Soft Tissues Using Indentation and Tensile Testing," *Jove-Journal of Visualized Experiments*, vol. 118, 2016.
- [4] W. Zhang, Y. Feng, C. Lee, K.L. Billiar, and M.S. Sacks, "A Generalized Method for the Analysis of Planar Biaxial Mechanical Data Using Tethered Testing Configurations," *J. Biomech. Eng.*, vol. 137, no. 6, pp. 13, 2015.
- [5] "Heart Failure," *National Heart, Lung, and Blood Institute*, 2017. Available: <https://www.nhlbi.nih.gov/health-topics/heart-failure>
- [6] "Causes of Heart Failure," *American Heart Association*, May 8, 2017. Available: http://www.heart.org/HEARTORG/Conditions/HeartFailure/CausesAndRisksForHeartFailure/Causes-of-Heart-Failure_UCM_477643_Article.jsp#.WuC4QIjwZPZ
- [7] I. S. Cohen and G. R. Gaudette, *Regenerating the Heart*. New York: Humana Press, 2011, pp. 536.
- [8] Geoffrey R. Mitchell and Ana Tojeira, "Role of Anisotropy in Tissue Engineering," *Procedia Engineering*, vol. 59, pp. 117-125, 2013.
- [9] M. S. Sacks, "Biaxial Mechanical Evaluation of Planar Biological Materials," *Journal of Elasticity and the Physical Science of Solids*, vol. 61, no. 1, pp. 199, 2000.
- [10] R. L. Mauck, B.M. Baker, N.L. Nerurkar, J.A. Burdick, W. Li, and R.S. Tuan, "Engineering on the straight and narrow: the mechanics of nanofibrous assemblies for fiber-reinforced tissue regeneration," *Tissue Engineering, Part B: Reviews*, vol. 15, pp. 171+, 2009.
- [11] M. R. Labrosse, R. Jafar, J. Ngu, and M. Boodhwani, "Planar biaxial testing of heart valve cusp replacement biomaterials: Experiments, theory and material constants," *Acta Biomaterialia*, vol. 45, , pp. 303-320, 2016.
- [12] M. S. Sirry, J.R. Butler, S.S. Patnaik, B. Brazile, R. Bertucci, and A. Claude, "Characterisation of the mechanical properties of infarcted myocardium in the rat under biaxial tension and uniaxial compression," *Journal of the Mechanical Behavior of Biomedical Materials*, vol. 63, pp. 252-264, 2016.
- [13] G. A. Holzapfel and R. W. Ogden, "On planar biaxial tests for anisotropic nonlinearly elastic solids. A continuum mechanical framework," *Mathematics and Mechanics of Solids*, vol. 14, no. 5, pp. 474-489, 2009.

- [14] V. Deplano, M. Boufi, O. Boiron, C. Guivier-Curien, Y. Alimi, and E. Bertrand, "Biaxial tensile tests of the porcine ascending aorta," *Journal of Biomechanics*, vol. 49, no. 10, pp. 2031-2037, 2016.
- [15] H. Fehervary, M. Smoljkić, J. Vander Sloten, and N. Famaey, "Planar Biaxial Testing of Soft Biological Tissue Using Rakes: A Critical Analysis of Protocol and Fitting Process," *Journal of the Mechanical Behavior of Biomedical Materials*, vol. 61, pp. 135-151, 2016.
- [16] Andrea Avanzini and Davide Battini, "Integrated Experimental and Numerical Comparison of Different Approaches for Planar Biaxial Testing of a Hyperelastic Material," *Advances in Materials Science and Engineering*, vol. 2016, pp. 1-12, 2016.
- [17] J. O. V. Delgadillo, S. Delorme and S. G. Hatzikiriakos, "Mechanical characterization of arteries: comparison of square and cruciform biaxial tests using inverse modeling technique," *Journal of Biomechanics*, vol. 39, pp. S324, 2006.
- [18] E. G. Roberts, E.L. Lee, D. Backman, J.A. Buczek-Thomas, S. Emani, and J.Y. Wong, "Engineering myocardial tissue patches with hierarchical structure-function," *Annals of Biomedical Engineering*, vol. 43, no. 3, pp. 762-773, 2015.
- [19] J. Grashow, A. Yoganathan and M. Sacks, "Biaxial Stress–Stretch Behavior of the Mitral Valve Anterior Leaflet at Physiologic Strain Rates," *Ann Biomed Eng*, vol. 34, no. 2, pp. 315-325, 2006.
- [20] "BioTester-Biaxial Testing," *CellScale*. Available: <http://cellscale.com/products/biotester/>.
- [21] "BioTester Biaxial Test System User Manual," *CellScale*. Available: <http://cellscale.com/wp-content/uploads/2017/01/BioTester-User-Manual-v7.4.pdf>.
- [22] "BioTester Brochure," *CellScale*. Available: <http://cellscale.com/wp-content/uploads/2016/11/BioTester-Brochure.pdf>.
- [23] Caleb Horst. Personal Communication, CellScale, September 8, 2017
- [24] R.T. Tranquillo, "INSTRON-SACKS PLANAR BIAxIAL SOFT TISSUE TESTING SYSTEM," *Materials Research Facilities Network*. Available: <http://www.mrfn.org/instruments/tissue-mechanics-lab/instron-sacks-planar-biaxial-soft-tissue-testing-system>.
- [25] Regents of the University of Minnesota, "Tissue Mechanics Library," *University of Minnesota: Department of Biomedical Engineering*, Feb. 15. Available: <http://bme.umn.edu/research/tissuemech.html>.
- [26] Regents of the University of Minnesota, "Instron-Sacks Planar Biaxial Soft Tissue Testing System Information," *University of Minnesota: Department of Biomedical Engineering*. Available: <http://bme.umn.edu/research/pdf/instron.pdf>.
- [27] International Organization for Standards, "Technical Product Documentation," *ISO*, 2015. Available: <https://www.iso.org/standard/56865.html>.

- [28] ASTM, "Standard Specification for Tensile Testing Machines for Textiles," *ASTM Compass*, 2011. Available: https://compass.astm.org/EDIT/html_historical.cgi?D76/D76M+11.
- [29] International Organization for Standards, "ISO 376:2011-Metallic materials," *ISO*, 2011. Available: <https://www.iso.org/standard/44661.html>.
- [30] ASTM, "Standard Guide for Characterization and Testing of Biomaterial Scaffolds Used in Tissue-Engineered Medical Products," *ASTM Compass*, 2013. Available: https://compass.astm.org/EDIT/html_annot.cgi?F2150+1.
- [31] International Organization for Standards, "ISO 7198:2016-Cardiovascular implants and extracorporeal systems," *ISO*, 2016. Available: <https://www.iso.org/standard/50661.html>.
- [32] ASTM, "Standard Test Method for Strength Properties of Tissue Adhesives in Tension," *ASTM Compass*, 2015. Available: [https://compass.astm.org/EDIT/html_annot.cgi?F2258+05\(2015\)](https://compass.astm.org/EDIT/html_annot.cgi?F2258+05(2015)).
- [33] "Reaction Torque Sensor - Flange," *Futek Advanced Sensor Technology*, 2016. Available: <http://www.futek.com/product.aspx?stock=FSH03981>.
- [34] H. Hung, C. Chong, A. Steinhart, J. Trexler, and K. Billiar, "Design of a biaxial test device for compliant tissue," 2005.
- [35] C. Suddath, "A Brief History of: Velcro," *Time*, 2010. Available: <http://content.time.com/time/nation/article/0,8599,1996883,00.html>.
- [36] "Important Considerations for Soft Tissue Testing," *Test Resources*, 2018. Available: <https://www.testresources.net/applications/industry/biomedical/tissue-engineering/important-considerations-for-soft-tissue-testing/>.
- [37] E. L. Bearer and L. Orci, "A simple method for quick-freezing," *Journal of Electron Microscopy Technique*, vol. 3, no. 2, pp. 233-241, 1986.
- [38] "How does a Force Transducer Work," *HBM*. Available: <https://www.hbm.com/en/6697/how-does-a-force-transducer-actually-work/>.
- [39] "Guide to the measurement of force," *The Institute of Measurement and Control*, London, UK, 2013.
- [40] "Force and weight measuring instruments," May. 2014.

Glossary

Anisotropy - (n.) the characteristic of exhibiting mechanical properties that vary depending upon the direction of load

ASTM - (n.) American Society for Testing and Materials; an international standards organization that develops and publishes voluntary consensus technical standards for a wide range of materials, products, systems, and services

Bending stiffness - (n.) resistance of a member against bending deformation

Biomimetic - (adj.) relating to or denoting synthetic methods that mimic biochemical processes

Compliance - (n.) the inverse of stiffness, flexibility

Contralateral - (adj.) of or pertaining to the other side

Displacement - (n.) the moving of something from its original position

Hysteresis - (n.) the phenomenon in which the value of a physical property lags behind changes in the effect causing it

ISO - (n.) International Organization for Standardization; an international standard-setting body composed of representatives from various national standards organizations

Lateral movement - (n.) range of motion in a plane, inversely related to bending stiffness

Modulus - (n.) also known as modulus of elasticity; a measure of the stiffness of a solid material

Pseudoplastic - (adj.) a material whose viscosity, or consistency due to internal resistance, decreases as shear stress increases

Scaffold - (n.) biomaterials, which act as templates for tissue regeneration, to guide the growth of new tissue

Shear - (n.) a strain in the structure of a substance produced by pressure, when its layers are laterally shifted in relation to each other

Strain - (n.) a measure of deformation within a material as a result of some applied force

Stress - (n.) a force per unit area applied to a material

Stress relaxation - (n.) a decrease in stress in a material being held under a constant strain for a finite amount of time

Tensile strength - (n.) a measurement of the maximum amount of force exerted on a material or member before failure

Viscoelasticity - (n.) the property of a substance of exhibiting both elastic and viscous behavior, the application of stress causing temporary deformation if the stress is quickly removed but permanent deformation if it is maintained

Appendix A:

Force Transducer Research

A transducer transforms a physical stimulus into a measurable output through a known relationship. Force transducers measure the resulting force in a specimen from a mechanically applied stress or strain, usually input as a value into mechanical testing equipment. Common force transducer applications include testing the force acting on an object, supplying reference measurements for comparison between measured values, bench testing, such as the ability of a product or material to withstand a certain force, and as force control in industrial machines and systems.

Strain Gauge Transducers

The most common force transducers are strain gauge force transducers that incorporate strain gauges in their internal structure. Strain gauges are conductors on a film. Under tension or compression, the length of these conductors change, resulting in a change in resistance which can determine the strain in the tested material. Resistance increases under strain and decreases in contraction [38]. This strain gauge is then firmly attached to a spring element. Through an applied force, like tension or compression, a mechanical stress is induced in the spring, resulting in a change in length and corresponding strain in both the spring and strain gauge. Strain gauge force transducers can be utilized for the measurement of forces in multiple directions, such as biaxial testing. In such multiaxial test methods, the Poisson's ratio calculates the relationship between transverse and axial strain. This ratio is directly dependent on the basic mass of a material; bulkier material requires higher forces. Therefore, higher nominal forces, or the intended maximum loads, in the force transducer are required.

The typical strain gauge force transducer incorporates four strain gauges oriented in a “ring”. This orientation is called a Wheatstone Bridge. The output of this circuit shows the change in resistance of the conductor of the strain gauge to determine the deformation of the spring of a known material. Then, the transducer can output the force induced that caused the measured deformation.

The strain gauge force transducer operates primarily on linear relationships. The force is directly proportional to stress, stress is proportional to strain, the change in resistance of the strain gauge conductor is proportionally dependent on the strain, and the output signal of Wheatstone bridge is proportional to that change in resistance. This transducer typically operates in a force range from 0.01 N to 50 MN depending on the specific type [39]. The strain gauge force transducer can measure both positive and negative forces of stress and strain, in tension or compression. These transducers are also calibrated once after production to last throughout the lifetime of each device. They need to exhibit reproducibility and robustness to continuously measure accurate and precise values of applied forces. To standardize the production and performance of force transducers, the International Organization for Standardization published ISO 376:2011 “Metallic materials -- Calibration of force-proving instruments used for the verification of uniaxial testing machines”, which details the needed requirements for the design, manufacture, and function of force transducers. Another relevant standard concerning similar requirements is VDI/VDE 2635 “Strain gauge standard for bonded electric resistance strain gauges, characteristics and testing conditions” [40].

Transducer Considerations

There are multiple kinds of force transducers and using transducers at all points of loading will reduce uncertainty. For any mechanical testing equipment that requires the use of a force transducer, the transducer must have adequate sensitivity to measure the applied force. It also must demonstrate an appropriate force range so that the tested material is not stretched to plastic deformation. Table A.1, compares several force transducers, including strain gauge and piezoelectric, and their ranges, uncertainties, and temperature sensitivities [39]. Various displacement transducers may be used with the gyroscopic and force balance load cells. Their performance limits will depend on the specific type of displacement transducer used, as denoted by the double asterisk, “**”, in the table.

Table A.1. Guide to Force Transducer Types and Characteristics

Device type	Typical range of rated capacities	Typical uncertainty (% of reading)	Typical temp. Sensitivity and operating range (% of reading/°C)
<i>Strain gauge load cells:</i> Semiconductor gauges Thin film gauges Foil gauges	0.01 N to 10 kN 0.1 N to 10 MN 5 N to 50 MN	0.2 to 1 0.02 to 1 0.02 to 1	0.02(-40°C to +80°C) 0.02(-40°C to +80°C) 0.01(-40°C to +80°C)
<i>Piezoelectric crystal</i>	1.5 mN to 120 MN	0.3 to 1	0.02(-190°C to +200°C)
<i>Hydraulic</i>	500 N to 5 MN	0.25 to 5	0.05(+5°C to +40°C)
<i>Pneumatic</i>	10 N to 500 kN	0.1 to 2	0.05(+5°C to +40°C)
<i>LVDT, capacitive, tuning-fork, vibrating wire</i>	10 mN to 1 MN	0.02 to 2	0.02(-40°C to +80°C)
<i>Magnetostrictive</i>	2 kN to 50 MN	0.5 to 2	0.04(-40°C to +80°C)
<i>Gyroscopic</i>	50 N to 250 N	0.001	0.0001(-10°C to +40°C)
<i>Force balance</i>	0.25 N to 20 N	0.0001	0.0001(-10°C to +40°C)

To determine the proper transducer for a mechanical test device, the range of force to be measured, the number of loading points, the direction of the forces, including tension or compression, the duration and rate of the application of the force, and the environmental conditions of testing must all be considered. Consequently, overloading the transducer can result in damaging the calibration intended to withstand the lifetime of the device.

Appendix B:

Hardware Testing

There are multiple ways to increase the sensitivity of the device. The team considered strain gauge, piezoelectric, and vibrating load cells for increased sensitivity. The new hardware must be able to produce and measure the low forces needed to test the soft tissue. The team is in the process of investigating the advantages and capabilities of the various load cells and force transducers available. The main focus for this research is to find the most accurate and sensitive components for the lower cost. Additionally, the team found it may be beneficial to obtain a newer computer to allow for reliable usage. Purchasing a new camera for improved displacement measurement may also be beneficial for results. Also, depending on the difficulty of loading into the existing device, the team may look into an automated loading device for improved ease of loading and improved loading time. After using the existing device, the team will decide which electronics are necessary to purchase.

To evaluate the functionality and accuracy of current hardware on the device, the team conducted several simple circuit tests to measure input and output of all force transducers, the signal conditioner, and the signal conditioner strain gauge modules.

The team tested all four Futek FT400 torque transducers for functionality through the use of a multimeter and programmable power source. These torque transducers work as resistors in a simple circuit after applying a load. The four torque transducers tested included two 20-oz. in transducers, with rated outputs of approximately 2.1 mV/V when a maximum load of around 2 Newtons is applied, and two 160-oz. in transducers, with rated outputs of approximately 1.8 mV/V when a maximum load of around 16 Newtons is applied. First, the team attached the positive and negative excitation leads of the programmable power source, set to output 10 V, to

the respective multimeter leads to ensure proper excitation. The expected output was 10 V, and the observed output was $10.00 \text{ V} \pm 0.002$; therefore, the team continued to test the transducers with this known excitation voltage from the calibrated power source.

The team connected one transducer to the multimeter and programmable power source through its four-wire cord. The positive excitation and negative excitation wires, red and black respectively, were attached to the corresponding nodes on the programmable power source. The power source was set to output 10 V of analog power to the transducer. The transducer's positive signal and negative signal leads, green and white respectively, were attached to the corresponding leads on the multimeter. The power source was turned on and the multimeter digital display was observed. Without loading, the multimeter read 0.000 V, which was expected. The force transducer was then loaded to approximately the maximum load using a slotted weight set with a hanger, in grams. The display was again observed. The expected output from each transducer, with an approximate rated output of 2 mV/V, at an excitation of 10 V was 2.000 mV. The observed output of all four torque transducers, after maximum loading, was $2.000 \text{ mV} \pm 0.020$. Through this simple circuit test, the team was able to verify that each transducer was functioning as intended and replacements do not need to be ordered for both 20-oz. in and 160-oz. in if those nominal loads are needed for future use in the machine.

Similarly, the team tested the signal conditioner block, SC-2345 in inputs 2/10 and 3/11, and the strain gauge modules, two SCC SG24 strain input signal conditioning modules Biax Strain Gauge and Strain Gauge 1. First, with a torque transducer attached to the corresponding nodes on Strain Gauge 1 in channel 3/11 within the signal conditioner block, positive excitation (red) in 1, negative excitation (black) in 2, positive signal (green) in 3, and negative signal (white) in 4, the input channels were tested using the same multimeter. The signal conditioner

specifications indicate an output excitation of 10 V, so the expected reading from attaching the multimeter to channels 1 and 2 was 10 V. The observed reading was $2.800 \text{ V} \pm 0.003$. The team removed Strain Gauge 1 and attached Biax Strain Gauge to the channel 3/11 in the signal conditioner block and repeated the test. The observed reading was $2.800 \text{ V} \pm 0.003$. The team removed Biax Strain Gauge and repeated the test with Strain Gauge 1 in channel 2/10 of the signal conditioning block. The observed excitation was the same, $2.800 \text{ V} \pm 0.003$. The team repeated the test using Biax Strain Gauge in channel 2/10 on the signal conditioning block and received the expected excitation of $10.000 \text{ V} \pm 0.002$.

The team then tested the output channels, 3 and 4, on Biax Strain Gauge in 2/10 within the signal conditioning block. After loading the transducer in the same manner as described previously, the expected display on the multimeter was 2 mV. The observed output was confirmed at $2.000 \text{ mV} \pm 0.020$. The team then tested the output of the strain gauge module by attaching the multimeter to the corresponding pins before entering the computer. The strain gauge modules have a specified gain factor of 100, so the expected output of the whole system was 0.2 V. After loading the force transducer following the same methods, the observed output was $0.200 \text{ V} \pm 0.004$. The team concluded that signal conditioner channel 2/10 with Biax Strain Gauge was functioning properly in excitation, force transducer signal input, and rated output. This hardware setup can now be used to test the software functioning of the device. Strain Gauge 1 and channel 3/11 of the signal conditioner failed to output the proper excitation for the system and should not be used unless the problem is further investigated or identified.

Appendix C:

Transducer Specifications

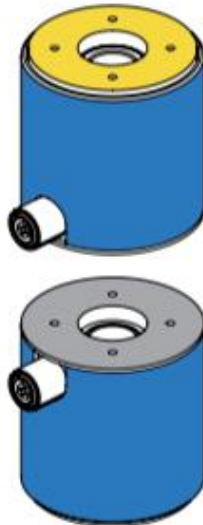
Brand	Name	Range	Force	Accuracy	Overload	Price
Torque						
Althen	E200 ORT	10mN*m	.138N	1% or .5%	200% safe	N/A
Althen	ATF315	10mN*m-5Nm	.138N-69N		125% safe, 150% max	N/A
Honeywell	Model 1700	.02Nm, .05Nm	.278N, .694N	0.25%	200% safe	N/A
Honeywell	Model 1103	10in-oz	.981N	0.09%	150%	\$6,315
Futek	TFF 400	10in-oz	.981N	(hysteresis/nonlinearity)	300%	\$1,200
Futek	TFF 400	5 in-oz	0.49N	(hysteresis/nonlinearity)	300%	\$1,200
Interface	5350	10in-oz		0.10%	200%	\$1,560



FEATURES

- Easily integrates into OEM applications
- Designed for Torque auditing
- Aluminum construction
- Built-in overload protection on lower ranges
- Strain gauge based

- Active End
- Fixed End
- Non-loading surface, do not contact



SPECIFICATIONS

PERFORMANCE

Nonlinearity	±0.2% of RO
Hysteresis	±0.2% of RO
Nonrepeatability	±0.05% of RO

ELECTRICAL

Rated Output (RO)	1 mV/V nom (5 in-oz) 2 mV/V nom (10 in-oz to 500 in-lb)
Excitation (VDC or VAC)	18 max
Bridge Resistance	350 Ohm nom (5 to 1000 in-oz) 700 Ohm nom (100 to 500 in-lb)
Connection	4 Pin LEMO® Receptacle (EGG.08.304.CLL)
Wiring/Connector Code	CC4

MECHANICAL

Weight (approximate)	9 oz [250 g]
Safe Overload	300% (5 to 1000 in-oz) of RO 150% (100 in-lb to 500 in-lb) of RO
Material	Aluminum
IP Rating	IP40

TEMPERATURE

Operating Temperature	-60 to 200°F (-50 to 93°C)
Compensated Temperature	60 to 160°F (15 to 72°C)
Temperature Shift Zero	±0.002% of RO/°F (0.0036% of RO/°C)
Temperature Shift Span	±0.002% of Load/°F (0.0036% of Load/°C)

CALIBRATION

Calibration Test Excitation	10 VDC
Calibration (standard)	5-pt CW
Calibration (available)	5-pt CW & CCW
Shunt Calibration Value	60.4 kOhm (10 to 1000 in-oz) 100 kOhm (5 in-oz, 100 to 500 in-lb)

Sensor Solution Source
Load · Torque · Pressure · Multi-Axis · Calibration · Instruments · Software
www.futek.com

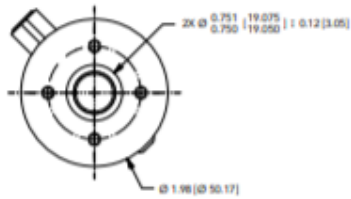
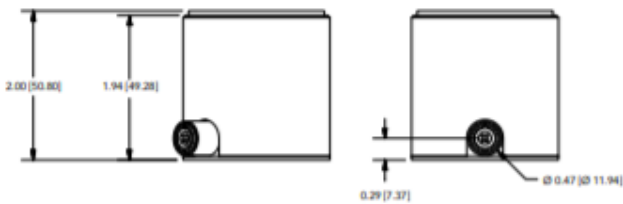
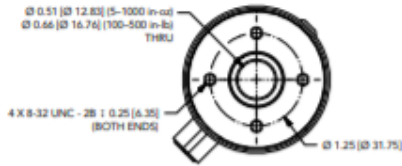


ROHS



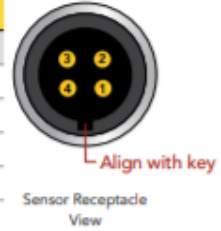
Model TFF400

DIMENSIONS inches [mm]



LEMO 4-PIN

PIN	COLOR	DESCRIPTION
1	Red	+ Excitation
2	Green	+ Signal
3	White	- Signal
4	Black	- Excitation



CAPACITIES

ITEM #	in-oz	Nm	Torsional Stiffness in-oz/rad	Natural Frequency (Hz)
FSH03981	5*	0.04	510	95
FSH03982	10*	0.07	510	95
FSH03984	50*	0.35	4200	260
FSH03985	160*	1.1	23000	504
FSH03986	400*	2.8	68300	860
FSH03987	1000*	7.1	232000	1590
FSH04015	100 in-lb	11	40000 in-lb/rad	2990
FSH04016	200 in-lb	22	67000 in-lb/rad	3860
FSH04017	500 in-lb	56	133000 in-lb/rad	5400

*With overload protection.
For high capacities refer to models TFF600 and TDF600-675.

Drawing Number: FI1457

FUTEK reserves the right to modify its design and specifications without notice.
Please visit <http://www.futek.com/salesterms> for complete terms and conditions.

10 Thomas, Irvine, CA 92618 USA
Tel: (949) 465-0900
Fax: (949) 465-0905
www.futek.com



RoHS



Appendix D:

System Diagram

The current biaxial test device is intended to measure force and displacement to analyze sub-failure properties of very soft, delicate, anisotropic biological and engineered materials. It is available for use by WPI faculty and students in Gateway Park. The current system is laid out as a biaxial tension test in a cross configuration with a force range of 0.001N to 2N. It follows a “patch system” setup in which each separate piece of hardware or software, such as the transducers, strain gauge modules, signal conditioner connector block, computer, and LabVIEW, communicates data or motion control to the next piece. This system is composed of various hardware and software, including:

- PC Computer: operating on Windows 2000
- LabVIEW '07: to program the device hardware to test the specimen and collect the needed data, obtained under a teaching license within a WPI contract with National Instruments (NI)
- Motor drive: NI MID-7604 to drive the motion control portion of the device
- Motion controller: NI PCI-7334 to operate the 4 compatible stepper motors
- Stepper motors: Advanced Microsystems 17-44-3MT to induce stress/strain in the test specimen by driving the tensile motion of the grips
- Camera: Sony XC-ST50 CCD to aerially visualize and track the displacement of 4 markers placed on the test specimen to control stress/strain in the sample
- Force transducers: 2 Futek rotary torque transducers, TF4400 (20 oz-in), used to measure the force induced in the specimen from the torque experienced by the arm attached to the transducer and specimen grips

- Amplifier: NI SCC-SG24 Strain Gauge Module to amplify the output of the force transducer by a gain factor for input into the AD board
- AD board: NI SC-2345 Signal Conditioning Connector Block to receive the amplified signal of the force transducers for transmission back to the computer and LabVIEW for analysis

This system is diagrammed in Fig. D.1 below with each arrow indicating the flow of data and each number representing the sequence of data flow.

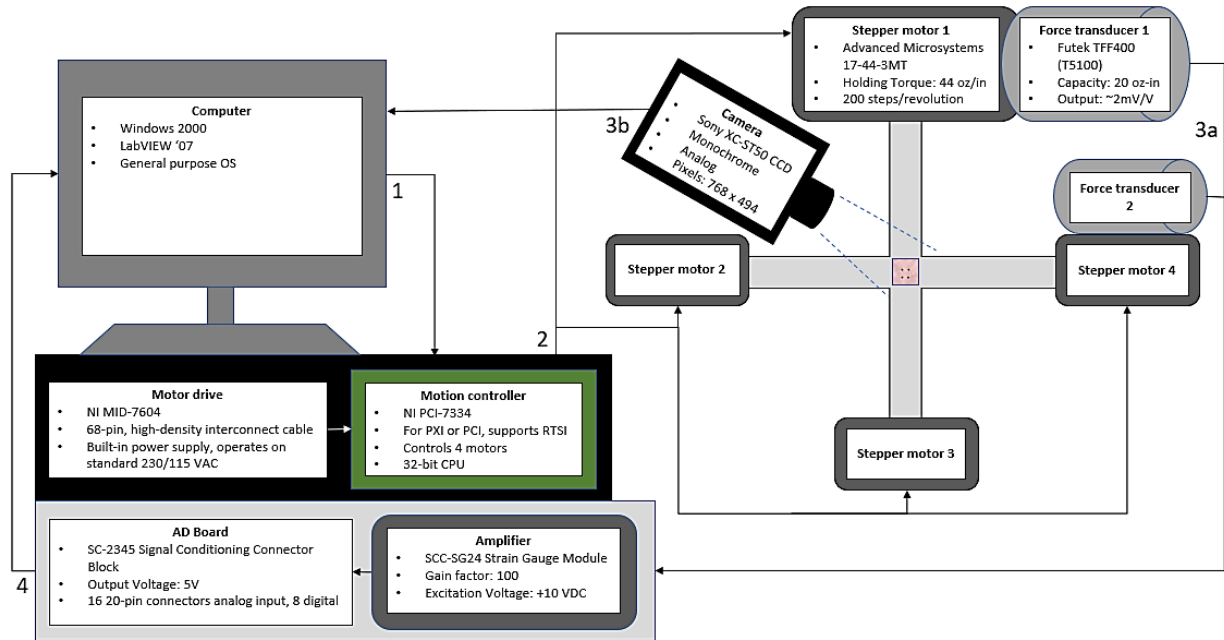


Fig. D.1. System Diagram (Figure D1 shows the flow of data, indicated by arrows, in the current biaxial test device system. The chronology of data flow is represented by the numbers next to each arrow on the diagram).

Future Recommendations



The team identified several main improvements to the current biaxial test device system including increasing device sensitivity, control, reliability, and quality of function and data collection. Through personal communication with National Instruments U.S. academic account

manager David Melendez, the research team identified the ideal device hardware and software updates to consider in the future to achieve the aforementioned improvements.

The first concern Mr. Melendez mentioned for the existing device is the age of some of the hardware. On this device, all of the signal conditioning (SC) units, including the strain gauge modules and signal conditioning connector block, have been phased out of National Instruments' products and would not be serviceable in the future. To increase the functioning lifespan of the device, Melendez recommended first updating these pieces with newer, more reliable technology offered by NI.

As far as improving data quality in terms of hardware and/or software, quality can be affected by sampling rate and resolution. Additionally, to improve sensitivity and control, future recommendations include synchronizing the stepper motors and actuators with the data acquisition system. This improvement minimizes the latency, or delayed response due to data flow from the separate pieces, in the current patch system.

The comprehensive quote of updates to the device obtained through personal communication with National Instruments U.S. Account Manager David Melendez is shown below in Fig. D.2.

Integrated Controller and Chassis			
Part Number	Description	Quantity	Price Per Unit
783830-01	cRIO-9063, 4-Slot Integrated Dual-Core Controller, Artix-7 FPGA	1	\$ 1,390
	STANDARD REPAIR COVERAGE	1	
			Subtotal: \$ 1,390
Modules			
Part Number	Description	Quantity	Price Per Unit
779781-01	NI 9219 4 Ch-Ch Isolated, 24-bit, ±60V,100S/s Universal AI Module	1	\$ 1,199
	STANDARD REPAIR COVERAGE	1	
196720-01	NI 9972 Backshell for 6-pos connector block (qty 4)	1	\$ 34
779944-01	NI 9512 1 Axis Stepper Drive Interface w/Encoder Feedback	2	\$ 582
	STANDARD REPAIR COVERAGE	2	
			Subtotal: \$ 2,397
System Accessories			
Part Number	Description	Quantity	Price Per Unit
 You have not selected any System Accessories. Select System Accessories.			
Services			
Part Number	Description	Quantity	Price Per Unit
SRV- CR5581739	STANDARD SERVICE PROGRAM FOR COMPACTRIO SYSTEMS	1	\$ 300.24
			Subtotal: \$ 300.24
Software			
Part Number	Description	Quantity	Price Per Unit
 You have not selected any software. Select software.			
			Total Price: \$ 4,087.24

* Price does not include local taxes (GST) or delivery charges.

Fig. D.2. Quoted hardware and software updates from David Melendez at National Instruments

Appendix E:

Relevant design calculations and experimental parameters

Using specimen dimensions, 1 cm x 1 cm x 1 mm, shown in Fig. E.1, the cross-sectional area of the specimen during testing was calculated.

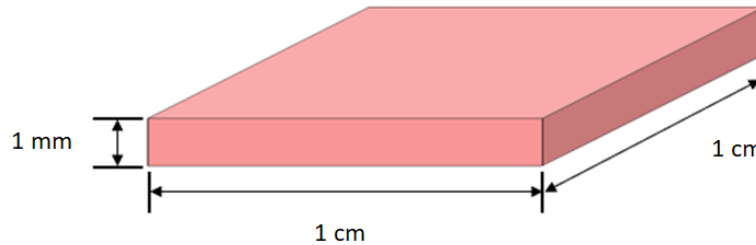


Fig. E1: Specimen Dimensions

$$A_{\text{cross-section}} = 10 \text{ mm} * 1 \text{ mm} = 10 \text{ mm}^2$$

Using this cross-sectional area, the nominal force range needed to test soft tissue specimens was calculated. A low threshold was determined through the use of the tensile strength, UTS, of the weakest soft tissue, arteries and veins: $UTS_{\text{artery/vein}} = 0.01 \text{ MPa}$. As ultimate tensile strength is calculated by force over cross-sectional area, the following equation was used, and the results are shown.

$$UTS = F / A \rightarrow F = UTS * A$$

$$0.01 \text{ MPa} * 10 \text{ mm}^2 = 0.1 \text{ N}$$

Because we are testing these soft tissues for sub-failure properties, the force transducers and load cells must have a sensitivity below this value, to mN. For an upper limit, one of the skin, was used; $UTS_{\text{ligament}} = 27.2 \text{ MPa}$.

$$UTS = F / A \rightarrow F = UTS * A$$

$$27.2 \text{ MPa} * 10 \text{ mm}^2 = 27.2 \text{ N}$$

Therefore, the approximate nominal range for our load cells and force transducers requires mN to approximately 680N.

Additionally, the device will measure sub-failure properties of stress, modulus of elasticity, and compliance. These properties can be determined through the following equations. Stress, σ , is measured by the force, F , over the cross-sectional area, A , upon which this force is applied in the specimen.

$$\sigma = F/A$$

Strain, ϵ , is calculated by the displacement of the specimen under an applied load, or the change in length, L , over the initial length, L_0 :

$$\epsilon = \Delta L / L_0$$

Modulus of elasticity, E , in the region plastic deformation of a material, is a linear relationship between an applied stress, σ , and the resulting strain, ϵ , in the material.

$$E = \sigma/\epsilon$$

Compliance, J , is directly related to modulus of elasticity, E .

$$J = 1/E$$

Another aspect of our gripping mechanism includes the bending stiffness of the grips themselves. Should the grips be too stiff, they may induce additional force on the test specimen and damage the specimen during testing. Should the grips have less than adequate stiffness, the grips may not induce enough force to effectively secure the specimen to experience the biaxial forces needed to test the specimen properties. To analyze the bending stiffness of alternative grips, such as CellScale's biorakes, we calculated the force required to deflect the rakes the maximum distance in the bath, measured to be 21mm. The following equations were used, in which P represents the force in N, L represents length in mm, r represents radius of each tine in

mm, E represents modulus of elasticity in MPa, I represents moment of inertia in mm⁴, Δ is the maximum deflection.

$$\Delta = PL^3/3EI$$

$$P = 3\Delta EI/L^3$$

For a rake with a circular cross section of radius r, the following equation was used to calculate moment of inertia, I.

$$I = \pi r^4/4$$

The calculated bending moments of CellScale’s circular cross-section biorakes of diameters .125mm, .15mm, and 0.25 mm are summarized in Table E.1 below.

Table E1. BioRake Bending Moment Calculations

variable	units	Biorake 1	Biorake 2	Biorake 3
r	mm	0.125	0.15	0.25
L	mm	30	30	30
E	MPa	190000	190000	190000
I	mm ⁴	0.000190429687	0.000394875	0.003046875
Δ	mm	21	21	21
P	N	0.08442382813	0.17506125	1.35078125
<i>Transducer resolution: 0.001N</i>				

To innovate a new gripping mechanism that improves upon the biorakes offered by CellScale, we will analyze the ideal shape and bending stiffness for our grips based on the desired maximum deflection.

Appendix F

Biaxial Device Testing

The device itself operates through multiple LabVIEW virtual instruments, or VIs. One VI controls the interpretation of the displacement images taken by the video camera positioned above the specimen while testing. Four marks are placed on the specimen prior to loading. Then, during testing, the video camera records the displacement of these marks as force is applied. The VI obtains an image signal from the camera through an NI PCI-1405 image acquisition board. The VI then uses image contrast to recognize the graphite markers; light pixels are shown in black while dark pixels are shown in red. There is a threshold range to allow the user to adjust the threshold range depending on the lighting. The VI also includes motor controls for the user to tighten and center the sample prior to testing. The virtual instrument front panel that interprets these images to calculate displacement, taken from the 2005 MQP report, is shown in Fig. F.1.

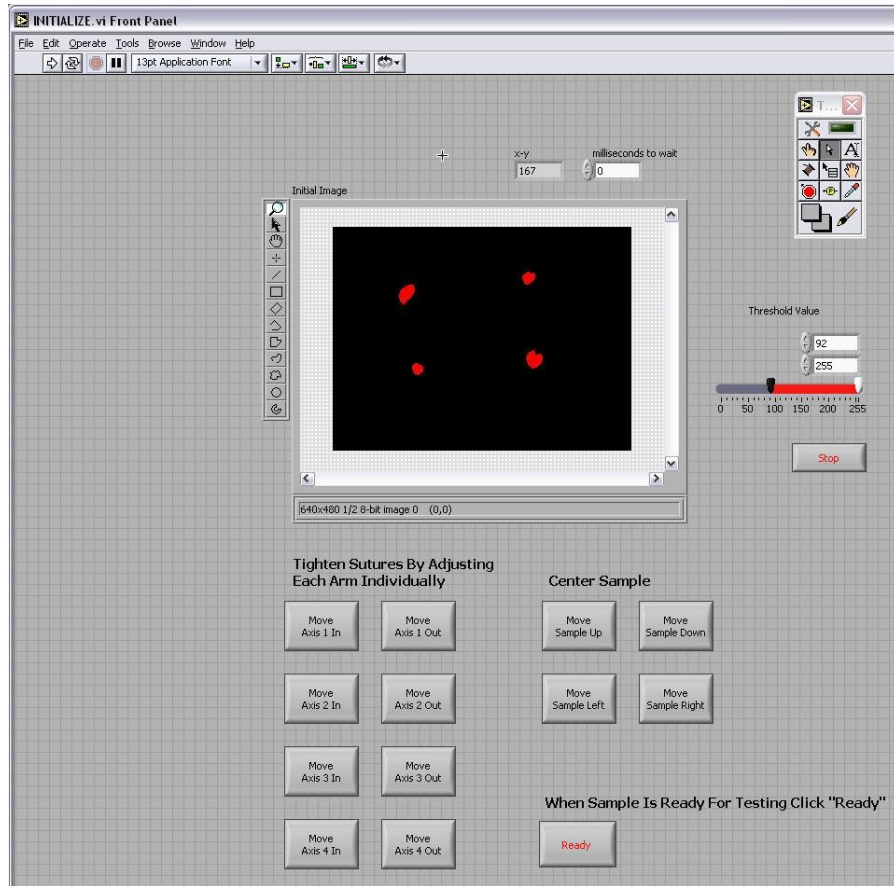


Fig. F.1: INITIALIZE.VI for Displacement Image Recognition

Image acquisition, IMAQ, then monitors the specimen's movement during loading. Centroids of the graphite markers, marked red, in the contrast image from the camera are tracked in real-time on the interface. The displacement of the centroids from their initial positions are then used to calculate average strain, which is plotted over strain in a stress-strain graph.

The second virtual instrument that is used to operate the machine is FINAL.VI. This virtual instrument performs the biaxial stretch test of the specimen while recording stress and strain. The two main inputs, from the user, to control the strain are percent strain and strain rate. Percent strain refers to the change in original dimensions that the user wants the specimen to experience. For example, to stretch the sample 10%, the user inputs a strain percent of 0.1. Strain

rate controls the rate at which the specimen is stretched, in s^{-1} . To stretch a the specimen by 10% in one second, the user inputs 0.1 into the strain rate.

Finally, data from the force transducers is used to measure the force applied to the specimen during testing. Data is collected from the transducers through the NI SC-2345 Signal Conditioning board. The FINAL.VI incorporates inputs from the user needed to calculate stress, shown in Fig. F.2.

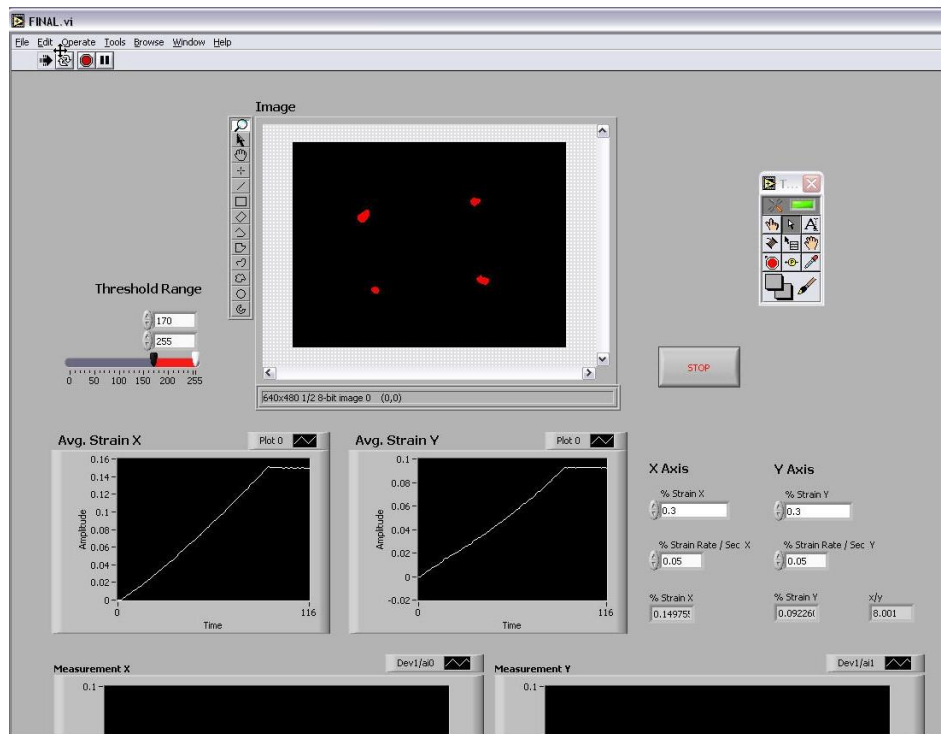


Fig. F.2: FINAL.VI

These inputs include the width of the sample, in both axes, the sample thickness, and the length of the arm attached to the transducer. Using these values, the VI then calculates the average stress in response to the force applied in a while loop to continuously graph the average stress in real-time. This graph is also displayed to the user on the interface.

Camera Acquisition

While the team was testing the LabVIEW code for the strain test, we came across a problem with the camera. The camera was not effectively locating the markers on the sample, which is problematic during testing, because the device is unable to monitor the movement of the sample. Several possibilities were discussed about why this was happening. The first was aliasing, which is when frequencies are sampled at a given rate, they give the same set of sample values or are indistinguishable from each other, so the camera needs to record at either a faster or slower rate to distinguish them. Another possibility discussed was that the contrast between the markers and the sample was not big enough. Because the latter was easier to test, the team tested it first. In order to do this, a sample of a lighter color was marked with black sharpie. We placed it in the testing position and we ran the program that provides the visual of the markers. The normal program was able to locate the markers perfectly. The contrast was enough so that we could see each marker without any discrepancy. The next test is to test a darker sample with light markers and see if it yields the same results. If it does, the team believes that the problem is mitigated and, unless additional problems arise, no further research or testing is required for our purposes.